Available online at http://scik.org
Commun. Math. Biol. Neurosci. 2021, 2021:22
https://doi.org/10.28919/cmbn/5077
ISSN: 2052-2541

AUTOMATED OPTIMAL VACCINATION AND TRAVEL-RESTRICTION CONTROLS WITH A DISCRETE MULTI-REGION SIR EPIDEMIC MODEL

HAMZA BOUTAYEB[1,*], SARA BIDAH[1], OMAR ZAKARY[1], MUSTAPHA LHOUS[2], MOSTAFA RACHIK[1]

[1]Laboratory of Analysis, Modeling and Simulation (LAMS), Department of Mathematics and Computer Science, Hassan II University of Casablanca, Faculty of Sciences Ben M'Sik, Sidi Othman, BP 7955, Casablanca, Morocco

[2]Laboratory of Modeling, Analysis, Control and Statistics, Department of Mathematics and Computer Science, Faculty of Sciences Ain Chock, Hassan II University of Casablanca, B.P 5366 Maarif Casablanca, Morocco

Abstract. Many mathematical models describing the evolution of infectious diseases underestimate the effect of the Spatio-temporal spread of epidemics. Currently, the COVID-19 epidemic shows the importance of taking into account the spatial dynamic of epidemics and pandemics. In this contribution, we consider a multi-region discrete-time epidemic model that describes the spatial spread of an epidemic within different geographical zones assumed to be connected with the movements of their populations. Based on the fact that there are several limitations in medical resources, the authorities and health decision-makers must define a threshold of infections in order to determine if a zone is epidemic or not yet. We propose a new approach of optimal control by defining new importance functions to identify affected zones and then the need for the control intervention. Numerical results are provided to illustrate our findings by applying this new approach in two adjacent regions of Morocco, the Casablanca-Settat and Rabat-Salé-Kénitra regions. We investigate different scenarios to show the most effective scenario, based on thresholds' values.

Keywords: automated vaccination; optimal control; multi-region; SIR model; epidemic model.

2010 AMS Subject Classification: 39A05, 39A45, 39A60, 93C35, 93C55.

*Corresponding author

E-mail address: hz.bouty@gmail.coml

Received October 01, 2020

1. INTRODUCTION

Among the fields of mathematical biology [1], mathematical epidemiology (ME) [2], that is to say, the construction and analysis of mathematical models describing the spread and control of infectious diseases, epidemics and pandemics, which has great utility influence. In fact, mathematical models of epidemics are currently commonly used in the evaluation of public health policies by national and international health agencies. In addition, an increasing number of articles in ME are published by reputable medical journals [4, 5, 6, 7, 8]. Epidemiological modeling and its applications have undergone a great evolution in recent decades, which has made it possible to analyze the evolution of epidemics from their population systems [12] and for different geographic areas [13, 14, 15].

A major assumption in many mathematical models of epidemics is that the population can be divided into a set of separate states. These states are defined according to the state of the disease. The simplest model, which calculates the theoretical number of people infected with a contagious disease in a closed population over time, described by Kermack and Mckendrick (1927), consists of three components: susceptible (S), infected (I) and recovered (R). The disease states are defined as follows:

• Susceptible: Individuals that have never been infected and can thus contract the disease. Once infected, they move to the infected state.

• Infected: Individuals that can transmit the disease to susceptible individuals. The time that individuals spend in the infected state is the infectious period; then they enter the recovered state.

• Recovered: Individuals in recovery are assumed to be immune for life [21].

Mathematical models have become important tools in analyzing the spread and control of infectious diseases. The model formulation process clarifies assumptions, variables and parameters. There have been many studies that have mathematically analyzed infectious diseases and several optimization approaches have been proposed to prove their effectiveness in the control of certain diseases, mainly, HIV, Ebola [14, 22, 23, 24, 25], ZIKA Virus [26], Malaria [27, 28], Influenza Pandemic [12], Cancer [29, 30], Tuberculosis [31, 32] and other diseases [33, 34, 14].

In the history of all these diseases, we can notice their spread from one region to another, and recently the COVID-19 pandemic from its epicenter of Wuhan in China has spread to all parts of the world, which makes taking into account the spatial spread of diseases more important during modeling processes.

The authors in [13] present the first work in the modeling and control of spatio-temporal spread of an epidemic using a multi-region SIR discrete-time model, as a generalization of the concept of classical models and aiming at a description of the evolution of pandemics, Zakary et al proposed a new approach of modeling of the spread of epidemics from one area to another using finite-dimensional models for the Spatio-temporal propagation of epidemics as an alternative of the partial derivatives models which are of infinite dimension. The authors also suggested some control strategies such as awareness-raising, vaccination, and travel-restriction approaches that could prevent specific infectious diseases such as HIV / AIDS, Ebola, or other epidemics in general [13, 15, 22, 14, 35], other researchers have shown the power and effectiveness of educational workshops and awareness programs in reducing the number of infected individuals [36, 37, 23].

In this paper, we propose a new optimal control approach mainly based on a multi-regions discrete-time model and a new form of multi-objective optimization criteria with importance functions and which is subject to multi-points boundary value optimal control problems. With more clarifications and essential details, we devise here a multi-regions discrete model for the study of the spread of an epidemic in M different zones, and analyze the effectiveness of vaccination (or awareness) and travel-restriction optimal control strategies when vaccination campaigns and/or travel restriction are applied in infected zones based on the number of infections. Here, we study the case when controls are applied to people who belong to all those regions and which are supposed to be reachable for every agent (nurse, doctor or media) who is responsible for the accomplishment of control strategies followed against the disease.

We consider an area as an infected zone if its number of infected individuals exceeds a threshold defined by the health decision-makers. Therefore, varying the values of this threshold and then simulating the infection situation for different values of these thresholds shows that it is necessary to think about reducing the time between the first infection and the implementation of

FIGURE 1. The geographical studied zone Ω: (a) Discretization on two regions Casablanca-Settat and Rabat-Sale-Kenitra. (b) Discretization of the two regions on provinces with numbers. (c) Discretization of the whole studied zone on provinces with names. (d) Zoom in to Casablanca and its neighbors.

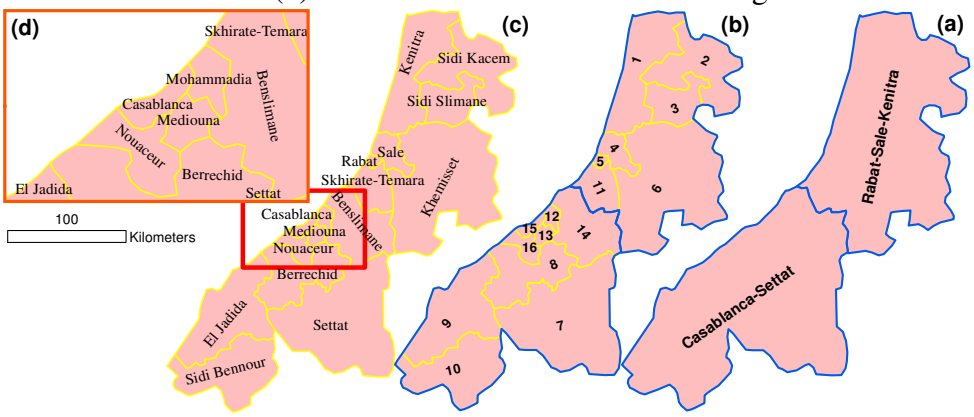

the control strategy. Unexpected results that in some situations the neighboring regions infected and its number of infections exceeds the threshold before the number of infections of the region source. This makes the implementation of the travel-restriction control strategy more important.

In our modeling approach we divided the studied area Ω into different zones that we call cells (or regions or zones). A cell $C_j \in \Omega$ can represent a city, a country or a larger domain. These cells are supposed to be connected by movements of their populations within the domain Ω. We define also a neighboring cells C_k of the cell C_j all zones connected with C_j via every transport mean, thus a cell $C_j \in \Omega$ can have more than one neighboring cell. Here, we suppose that a cell can be infected due to movements of infected people which enter from its neighboring zones.

We carry out the map of the studied area and then we use different threshold values in the controlled multi-region SIR model to simulate the epidemic spread within the Casablanca-Settat region and Rabat-Sale-Kenitra region illustrated in the Fig.1, by combining the ArcGIS and Matlab programs.

The paper is organized as follows: Section 2. presents the discrete-time multi-region SIR epidemic system. In Section 3., we announce theorems of the existence and characterization of the sought optimal controls functions related to the optimal control approach we propose. Finally, in section 4., we provide simulations of the numerical results applied to the Casablanca-Settat region and Rabat-Sale-Kenitra region as domain of interest. Section 5 concludes.

2. Model Description and Definitions

Based on modeling assumptions of the reference [13], we assume that there are M geographical zones denoted C_j (sub-domains, regions, cities, towns ...) of the studied domain Ω

$$\Omega = \bigcup_{j=1}^{M} C_j$$

Where C_j can represent a city, a country or a larger domain. For instance, in the Fig.1 we show an example of geographical discretization of tow regions of Morocco, that is, Casablanca-Settat and Rabat-Sale-Kenitra with 16 zones. We define $V(C_j)$, the vicinity set, composed by all neighboring cells of C_j given by

$$V(C_j) = \left\{C_k \in \Omega \ / \ C_j \cap C_k \neq \emptyset\right\}, C_j \notin V\left(C_j\right)$$

Where $C_j \cap C_k \neq \emptyset$ means that there exists at least one mean of transport between C_j and C_k. Note that this definition of $V(C_j)$ is more general where it defines a more general form of vicinity regardless the geographical location of zones.

The multi-regional discrete-time SIR model associated to C_j when there is no control introduced yet is then

$$S_{i+1}^{C_j} = S_i^{C_j} - \beta_{jj}\frac{I_i^{C_j}}{N_i^{C_j}}S_i^{C_j} - \sum_{C_k \in V(C_j)} \beta_{jk}\frac{I_i^{C_k}}{N_i^{C_j}}S_i^{C_j} + \left(N_i^{C_j} - S_i^{C_j}\right)d_j \tag{1}$$

$$I_{i+1}^{C_j} = I_i^{C_j} + \beta_{jj}\frac{I_i^{C_j}}{N_i^{C_j}}S_i^{C_j} + \sum_{C_k \in V(C_j)} \beta_{jk}\frac{I_i^{C_k}}{N_i^{C_j}}S_i^{C_j} - \gamma_j I_i^{C_j} - d_j I_i^{C_j} - \alpha_j I_i^{C_j} \tag{2}$$

$$R_{i+1}^{C_j} = R_i^{C_j} + \gamma_j I_i^{C_j} - d_j R_i^{C_j} \tag{3}$$

where the disease transmission coefficient $\beta_{jk} > 0$ is the proportion of adequate contacts in domain C_j between a susceptible from C_j $(j = 1,...,M)$ and an infective from another domain C_k, d_j is the birth and death rate and γ_j is the recovery rate ans α_j is the proportion of mortality due to the disease. The biological background requires that all parameters be non-negative. $S_i^{C_j}$, $I_i^{C_j}$ and $R_i^{C_j}$ are the numbers of individuals in the susceptible, infective, and recovered

Nb	Zone	Population	Nb	Zone	Population	Nb	Zone	Population	Nb	Zone	Population
1	KINETRA	1061435	5	RABAT	577827	9	EL JADIDA	786716	13	MEDIOUNA	172680
2	SIDI KACEM	522270	6	KHEMISSAT	542221	10	SIDI BENNOUR	452448	14	BENSLIMANE	233123
3	SIDI SLIMANE	320407	7	SETTAT	634184	11	SKHIRATE-TEMARA	574543	15	CASABLANCA	3032116
4	SALE	982163	8	BERRCHID	484518	12	MOHEMMEDIA	404648	16	NOUACEUR	333604

TABLE 1. Populations of the two regions Casablanca-Settat and Rabat-Sale-Kenitra illustrated in Fig.1.

compartments of C_j at time i, respectively, and $N_i^{C_j} = S_i^{C_j} + I_i^{C_j} + R_i^{C_j}$ is the population size corresponding to domain C_j at time i. It is clear that the population size is not constant for all $i \geq 0$.

3. TRAVEL-RESTRICTION AND VACCINATION CONTROLS

3.1. Presentation of the model with controls. In this section, we introduce a control variable $u_i^{C_j}$ that characterizes the effectiveness of the vaccination in the above mentioned model (1-3). This control in some situations can represent the effect of the awareness and media programs [14, 22].

In almost all infectious diseases, the authorities determine the threshold of risk based on many factors, such as availability of medical equipment, budgets, and medical personnel ... Thus, they can wait some time to see the course of events before the intervention. If the number of casualties exceeds a predefined limit, decision-makers have no choice but to start trying to control the situation. This motivate us to define a Boolean function $\varepsilon_i^{C_j}$ ($\varepsilon_i^{C_j} = 1$ or $\varepsilon_i^{C_j} = 0$) associated to the domain C_j, that will be called the importance function of C_j. Where $\varepsilon_i^{C_j}$ is either equaling to 1, in the case when the number of infections in the cell C_j at instant i is greater than or equal to the threshold of vaccination $\mathscr{I}_V^{C_j}$ defined by the authorities and health decision-makers, or $\varepsilon_i^{C_j} = 0$ otherwise. Therefore, we define the importance function associated to the vaccination control $\varepsilon_{v,i}^{C_j}$ by the Heaviside step function H as follows

$$\varepsilon_{v,i}^{C_j} = H\left(I_i^{C_j} - \mathscr{I}^{C_j}\right) = \begin{cases} 0 & I_i^{C_j} < \mathscr{I}_V^{C_j} \\ 1 & I_i^{C_j} \geq \mathscr{I}_V^{C_j} \end{cases}$$

In the case of epidemics and pandemics, and in the absence of effective treatment, governments tend to take non-drug measures to reduce the number of victims. Travel restrictions, self-isolation and social isolation are the most commonly used non-drug measures in such situations. Therefore, we introduce a second control variable $v_i^{C_j}$ that characterizes the travel-restriction operation which aims to restrict movements of people coming from neighboring zones $C_k \in V(C_j)$ to the affected zone C_j, in order to facilitate the categorization of people depending on their cases. Thus, we define a threshold based on the number of infections to determine affected zones. Then, $\mathscr{I}_T^{C_j}$ is the tolerable number of infections in the zone C_j before the closure of this zone, i.e. if the number of infections $I_i^{C_j}$ in C_j exceeds $\mathscr{I}_T^{C_j}$, C_j is called an affected zone and then the travel-restriction will be applied. Therefore, the importance function associated to the travel-restriction control $\varepsilon_{T,i}^{C_j}$ is also defined by the Heaviside step function H as follows

$$\varepsilon_{T,i}^{C_j} = H\left(I_i^{C_j} - I_{sT}^{C_j}\right) = \begin{cases} 0 & I_i^{C_j} < \mathscr{I}_T^{C_j} \\ 1 & I_i^{C_j} \geq \mathscr{I}_T^{C_j} \end{cases}$$

Based on all these considerations, for a given zone $C_j \in \Omega$, the model is given by the following equations

$$\begin{aligned} S_{i+1}^{C_j} &= S_i^{C_j} - \beta_{jj} \frac{I_i^{C_j}}{N_i^{C_j}} S_i^{C_j} - \sum_{C_k \in V(C_j)} \left(1 - \varepsilon_{T,i}^{C_j} v_i^{C_j}\right) \beta_{jk} \frac{I_i^{C_k}}{N_i^{C_j}} S_i^{C_j} \\ &\quad + \left(N_i^{C_j} - S_i^{C_j}\right) d_j - \varepsilon_{v,i}^{C_j} u_i^{C_j} S_i^{C_j} \end{aligned} \tag{4}$$

$$\begin{aligned} I_{i+1}^{C_j} &= I_i^{C_j} + \beta_{jj} \frac{I_i^{C_j}}{N_i^{C_j}} S_i^{C_j} + \sum_{C_k \in V(C_j)} \left(1 - \varepsilon_{T,i}^{C_j} v_i^{C_j}\right) \beta_{jk} \frac{I_i^{C_k}}{N_i^{C_j}} S_i^{C_j} \\ &\quad - \gamma_j I_i^{C_j} - d_j I_i^{C_j} - \alpha_j I_i^{C_j} \end{aligned} \tag{5}$$

$$R_{i+1}^{C_j} = R_i^{C_j} + \gamma_j I_i^{C_j} - d_j R_i^{C_j} + \varepsilon_{v,i}^{C_j} u_i^{C_j} S_i^{C_j} \tag{6}$$

Our goal is obviously to try to minimize the population of the susceptible and infected groups and the cost of vaccinations and travel-restriction in all affected zones.

3.2. An optimal control approach. We devise in this paper an automated optimal control approach for each region with different importance functions $\varepsilon_{*,i}^{C_j}$, $j = 1, ..., M$. We characterize

optimal controls that minimize the number of the infected people and maximize the ones in the recovered category for all affected regions. Then, we are interested by minimizing the functional

$$J(u,v) = \sum_{k=1}^{M} max(\varepsilon_{v,i}^{C_j}, \varepsilon_{T,i}^{C_j}) J_k(u^{C_k}, v^{C_k}) \tag{7}$$

where $J_j(u^{C_k}, v^{C_k})$ is given by

$$J_j(u^{C_j}, v^{C_j}) = (\alpha_j^I I_N^{C_j} - \alpha_j^R R_N^{C_j}) + \sum_{i=0}^{N-1} \Big(\alpha_j^I I_i^{C_j} - \alpha_j^R R_i^{C_j} + \varepsilon_{v,i}^{C_j} \frac{A_j}{2} (u_i^{C_j})^2 + \varepsilon_{T,i}^{C_j} \frac{B_j}{2} (v_i^{C_j})^2\Big) \tag{8}$$

(9)

where $A_j > 0, B_j > 0, \alpha_I^{C_j} > 0, \alpha_R^{C_j} > 0$ are the weight constants of controls, the infected and the recovered populations in the region C_j respectively, and $u = \left(u^{C_1}, ..., u^{C_M}\right)$ with $u^{C_j} = \left(u_0^{C_j}, ..., u_{N-1}^{C_j}\right)$, and $v = \left(v^{C_1}, ..., v^{C_M}\right)$ with $v^{C_j} = \left(v_0^{C_j}, ..., v_{N-1}^{C_j}\right)$.

Our goal is to minimize the infected individuals, minimize the systemic costs of vaccinations and travel-restriction attempting to increase the number of recovered people in each zone $C_j \in \Omega$. In other words, we are seeking optimal controls u^* and v^* such that

$$J(u^*, v^*) = min\{J(u,v) / u \in U, v \in V\}$$

where U and V are the control sets defined by

$$U = \Big\{u \text{measurable} / u_{min}^{C_j} \leq u_i^{C_j} \leq u_{max}^{C_j}, i = 0, ..., N-1, j = 1, ..., M\Big\} \tag{10}$$

$$V = \Big\{v \text{measurable} / v_{min}^{C_j} \leq v_i^{C_j} \leq v_{max}^{C_j}, i = 0, ..., N-1, j = 1, ..., M\Big\} \tag{11}$$

where $0 < u_{min}^{C_j} < u_{max}^{C_j} < 1$ and $0 < v_{min}^{C_j} < v_{max}^{C_j} < 1$, By using Pontryagin's Maximum Principle [38] we derive necessary conditions for our optimal controls. For this purpose we define the Hamiltonian as

$$
\begin{aligned}
\mathscr{H} \quad = \quad & \sum_{k=1}^{M} max(\varepsilon_{v,i}^{C_k}, \varepsilon_{T,i}^{C_k}) \left(\alpha_k^I I_i^{C_k} - \alpha_k^R R_i^{C_k} \right. \\
& \left. + \varepsilon_{v,i}^{C_k} \frac{A_k}{2} \left(u_i^{C_k} \right)^2 + \varepsilon_{T,i}^{C_k} \frac{B_k}{2} (v_i^{C_k})^2 \right) \\
& + \sum_{j=1}^{M} max(\varepsilon_{v,i}^{C_j}, \varepsilon_{T,i}^{C_j}) \left(\zeta_{1,i+1}^j \left[S_i^{C_j} - \beta_{jj} \frac{I_i^{C_j}}{N_i^{C_j}} S_i^{C_j} - \sum_{C_k \in V(C_j)} \left(1 - \varepsilon_{T,i}^{C_j} v_i^{C_j} \right) \beta_{jk} \frac{I_i^{C_k}}{N_i^{C_j}} S_i^{C_j} \right. \right. \\
& \left. + \left(N_i^{C_j} - S_i^{C_j} \right) d_j - \varepsilon_{v,i}^{C_j} u_i^{C_j} S_i^{C_j} \right] \\
& + \zeta_{2,i+1}^j \left[I_i^{C_j} + \beta_{jj} \frac{I_i^{C_j}}{N_i^{C_j}} S_i^{C_j} + \sum_{C_k \in V(C_j)} \left(1 - \varepsilon_{T,i}^{C_j} v_i^{C_j} \right) \beta_{jk} \frac{I_i^{C_k}}{N_i^{C_j}} S_i^{C_j} \right. \\
& \left. - \gamma_j I_i^{C_j} - d_j I_i^{C_j} - \alpha_j I_i^{C_j} \right] \\
& \left. + \zeta_{3,i+1}^j \left[R_i^{C_j} + \gamma_j I_i^{C_j} - d_j R_i^{C_j} + \varepsilon_{v,i}^{C_j} u_i^{C_j} S_i^{C_j} \right] \right)
\end{aligned} \tag{12}
$$

Theorem 1.

Given optimal controls u^{C_j*}, v^{C_j*} and solutions S^{C_j*}, I^{C_j*} and R^{C_j*}, there exists $\zeta_{k,i}^j$, $i = 1, ..., N$, $k = 1, 2, 3$, the adjoint variables satisfying the following equations

$$
\begin{aligned}
\Delta\zeta_{1,i}^j \quad = \quad & -max(\varepsilon_{v,i}^{C_j}, \varepsilon_{T,i}^{C_j}) \left[\left(1 - \beta_{jj} \frac{I_i^{C_j}}{N_i^{C_j}} - \sum_{C_k \in V(C_j)} \left(1 - \varepsilon_{T,i}^{C_j} v_i^{C_j} \right) \beta_{jk} \frac{I_i^{C_k}}{N_i^{C_j}} - d_j - \varepsilon_{v,i}^{C_j} u_i^{C_j} \right) \zeta_{1,i+1}^j \right. \\
& \left. + \left(\beta_{jj} \frac{I_i^{C_j}}{N_i^{C_j}} + \sum_{C_k \in V(C_j)} \left(1 - \varepsilon_{T,i}^{C_j} v_i^{C_j} \right) \beta_{jk} \frac{I_i^{C_k}}{N_i^{C_j}} \right) \zeta_{2,i+1}^j + \varepsilon_{v,i}^{C_j} u_i^{C_j} \zeta_{3,i+1}^j \right]
\end{aligned} \tag{13}
$$

$$
\begin{aligned}
\Delta\zeta_{2,i}^j \quad = \quad & -max(\varepsilon_{v,i}^{C_j}, \varepsilon_{T,i}^{C_j}) \left[\alpha_j^I + \beta_{jj} \frac{S_i^{C_j}}{N_i^{C_j}} \left(\zeta_{2,i+1}^j - \zeta_{1,i+1}^j \right) \right. \\
& \left. + \left(1 - \gamma_j - d_j - \alpha_j \right) \zeta_{2,i+1}^j + \gamma_j \zeta_{3,i+1}^j \right]
\end{aligned} \tag{14}
$$

$$
\Delta\zeta_{3,i}^j = -max(\varepsilon_{v,i}^{C_j}, \varepsilon_{T,i}^{C_j}) \left[-\alpha_j^R + \left(1 - d_j \right) \zeta_{3,i+1}^j \right] \tag{15}
$$

where $\zeta^j_{1,N}=0, \zeta^j_{2,N}=max(\varepsilon^{C_j}_{v,i},\varepsilon^{C_j}_{T,i})\alpha^I_j, \zeta^j_{3,N}=-max(\varepsilon^{C_j}_{v,i},\varepsilon^{C_j}_{T,i})\alpha^R_j$ are the transversality conditions. In addition

$$u^*=\left(u^{C_1*},...,u^{C_p*}\right) \text{ and } v^*=\left(v^{C_M*},...,u^{C_M*}\right)$$

where $u^{C_j*}=\left(u_0^{C_j*},...,u_{N-1}^{C_j*}\right)$ and $v^{C_j*}=\left(v_0^{C_j*},...,v_{N-1}^{C_j*}\right)$ are given by

$$\begin{aligned} u_i^{C_j*} &= min\left\{max\left\{u_{min}^{\Omega_j}, max(\varepsilon^{C_j}_{v,i},\varepsilon^{C_j}_{T,i})\frac{\left(\zeta^j_{1,i+1}-\zeta^j_{3,i+1}\right)S_i^{C_j*}}{A_j}\right\}, u_{max}^{C_j}\right\} \; if\; \varepsilon^{C_j}_{v,i}=1 \\ u_i^{C_j*} &= 0, \quad \text{Otherwise} \end{aligned} \tag{16}$$

$$\begin{aligned} v_i^{C_j*} &= min\left\{max\left\{v_{min}^{C_j^k}, max(\varepsilon^{C_j}_{v,i},\varepsilon^{C_j}_{T,i})\frac{(\zeta^j_{2,i+1}-\zeta^j_{1,i+1})}{B_j}\sum_{C_k\in V(C_j)}\beta_{jk}\frac{I_i^{C_k}}{N_i^{C_j}}S_i^{C_j}\right\}, v_{max}^{C_j^k}\right\} \; if\; \varepsilon^{C_j}_{T,i}=1 \\ v_i^{C_j*} &= 0, \text{Otherwise.} \end{aligned} \tag{17}$$

Proof. Using Pontryagin's Maximum Principle [38], we obtain the following adjoint equations

$$\begin{aligned} \Delta\zeta^{C_j}_{1,i} &= -\frac{\partial\mathscr{H}}{\partial S_i^{C_j}} = -max(\varepsilon^{C_j}_{v,i},\varepsilon^{C_j}_{T,i})\left[\left(1-\beta_{jj}\frac{I_i^{C_j}}{N_i^{C_j}}-\sum_{C_k\in V(C_j)}\left(1-\varepsilon^{C_j}_{T,i}v_i^{C_j}\right)\beta_{jk}\frac{I_i^{C_k}}{N_i^{C_j}}-d_j-\varepsilon^{C_j}_{v,i}u_i^{C_j}\right)\zeta^j_{1,i+1}\right. \\ &\quad \left.+\left(\beta_{jj}\frac{I_i^{C_j}}{N_i^{C_j}}+\sum_{C_k\in V(C_j)}\left(1-\varepsilon^{C_j}_{T,i}v_i^{C_j}\right)\beta_{jk}\frac{I_i^{C_k}}{N_i^{C_j}}\right)\zeta^j_{2,i+1}+\varepsilon^{C_j}_{v,i}u_i^{C_j}\zeta^j_{3,i+1}\right] \\ \Delta\zeta^{C_j}_{2,i} &= -\frac{\partial\mathscr{H}}{\partial I_i^{C_j}} = -max(\varepsilon^{C_j}_{v,i},\varepsilon^{C_j}_{T,i})\left[\alpha^I_j+\beta_{jj}\frac{S_i^{C_j}}{N_i^{C_j}}\left(\zeta^j_{2,i+1}-\zeta^j_{1,i+1}\right)\right. \\ &\quad \left.+(1-\gamma_j-d_j-\alpha_j)\zeta^j_{2,i+1}+\gamma_j\zeta^j_{3,i+1}\right] \\ \Delta\zeta^{C_j}_{3,i} &= -\frac{\partial\mathscr{H}}{\partial R_i^{C_j}} = -max(\varepsilon^{C_j}_{v,i},\varepsilon^{C_j}_{T,i})\left[-\alpha^R_j+(1-d_j)\zeta^j_{3,i+1}\right] \end{aligned}$$

with $\zeta^{C_j}_{1,N}=0, \zeta^{C_j}_{2,N}=\varepsilon_i^{C_j}\alpha_I^{C_j}, \zeta^{C_j}_{3,N}=-\varepsilon_i^{C_j}\alpha_R^{C_j}$. To obtain the optimality conditions we take the variation with respect to control $u_i^{C_j}$ and $v_i^{C_j}$ and solve for u^{C_j} and v^{C_j} respectively we get

$$u_i^{C_j*} = max(\varepsilon^{C_j}_{v,i},\varepsilon^{C_j}_{T,i})\frac{\left(\zeta^j_{1,i+1}-\zeta^j_{3,i+1}\right)S_i^{C_j*}}{A_j}$$

□

Parameter	Description	Value
β	Infection rate	0.001
d	Birth and death rate	0.00001
γ	Recovery rate	0.00001
α	Death due to the infection	0.0001

TABLE 2. Parameters values of β, d, α and γ utilized for the resolution of all multi-regions discrete systems and then leading to simulations obtained from Fig.3 to Fig.38, with the initial populations given in Table 1.

$$v_i^{C_j^k *} = max(\varepsilon_{v,i}^{C_j}, \varepsilon_{T,i}^{C_j}) \frac{(\zeta_{2,i+1}^j - \zeta_{1,i+1}^j)}{B_j} \sum_{C_k \in V(C_j)} \beta_{jk} \frac{I_i^{C_k}}{N_i^{C_j}} S_i^{C_j}$$

By taking bounds of controls from U and V we get the result.

4. NUMERICAL RESULTS

In this section, we present numerical simulations associated to the above mentioned optimal control problem. We write a code in $MATLAB^{TM}$ and simulated our results for several scenarios. The optimality systems is solved based on an iterative discrete scheme that converges following an appropriate test similar the one related to the Forward-Backward Sweep Method (FBSM). The state system with an initial guess is solved forward in time and then the adjoint system is solved backward in time because of the transversality conditions. Afterwards, we update the optimal control values using the values of state and co-state variables obtained at the previous steps. Finally, we execute the previous steps till a tolerance criterion is reached.

4.1. Area of interest. We chose the Casablanca-Settat region and the Rabat-Sale-Kenitra region as the studied area Ω in this paper because we are convinced that we can find some useful data to support our work. They are the most populated and dynamic regions of Morocco, which contain the Rabat city as the capital of Morocco and the seventh largest city in the country with an urban population of around 580,000 inhabitants (2014) and a metropolitan population of more than 1.2 million inhabitants. It is also the capital of the administrative region of Rabat-Sale-Kenitra. They contain also the Casablanca city as the economic and industrial capital of

Morocco because with its demographic growth and continuous development of the industrial sector, and the 14 other provinces (see Fig.1), in order to illustrate the objective of our work.

Fig.1 illustrates an example of discrete geographical zones of Casablanca-Settat and Rabat-Sale-Kenitra regions (Morocco) where $M = 16$, this image was originally made based on information from [39, 40, 41].

4.2. Geographical vicinity. A shape-file is a simple, non topological format for storing the geometric location and attribute information of geographic features. Geographic features in a shape-file can be represented by points, lines, or polygons (areas). The workspace containing shape-files may also contain database tables, which can store additional attributes that can be joined to a shape-file's features [42]. ArcMap is a central application used in ArcGIS software, where we can view and explore GIS database for our study area, and where we assign symbols and create map layouts for printing or publication. In this application we can represent geographic information as a set of layers and other elements in a map. Common map elements of a map include the data frame containing the map layers for a given extent [43]. Neighborhood tools create output values for each cell location based on the location value and the values identified in a specified neighborhood [44]. We use this tool to create the neighborhood $V(C_j)$ of each separated zone C_j within the area of interest Ω. For instance

$$V(C_{15}) = \{C_{12}, C_{13}, C_{16}\}$$

4.3. Initialization. Without loss of generality, we set the same infection thresholds for all zones, therefore, hereafter we note $\mathscr{I}_T^{C_j}$ as $\mathscr{I}^{\mathscr{T}}{}_{min}$ and $\mathscr{I}_V^{C_j}$ as $\mathscr{I}^{\mathscr{V}}{}_{min}$. We suppose as initial states in the area of interest Ω the following values:

Susceptible: The real populations given in Table 1.

Infected: 100 infections only in the city of Casablanca, and 0 for the others.

Recovered: We assume that $i = 0$ represents the first appearance of the epidemic, therefore, there are no recovered individuals.

Parameters We use the parameters' values given in Table 2 for all zones.

Fig.2 represents the initial states of the multi-region SIR model of the 16 regions (zones) defined in the Fig.1. Fig.2 (a) defines in color the number of the initial states of susceptible in

FIGURE 2. Initial states. (a) Susceptible population. (b) Infected population. (c) Recovered population.

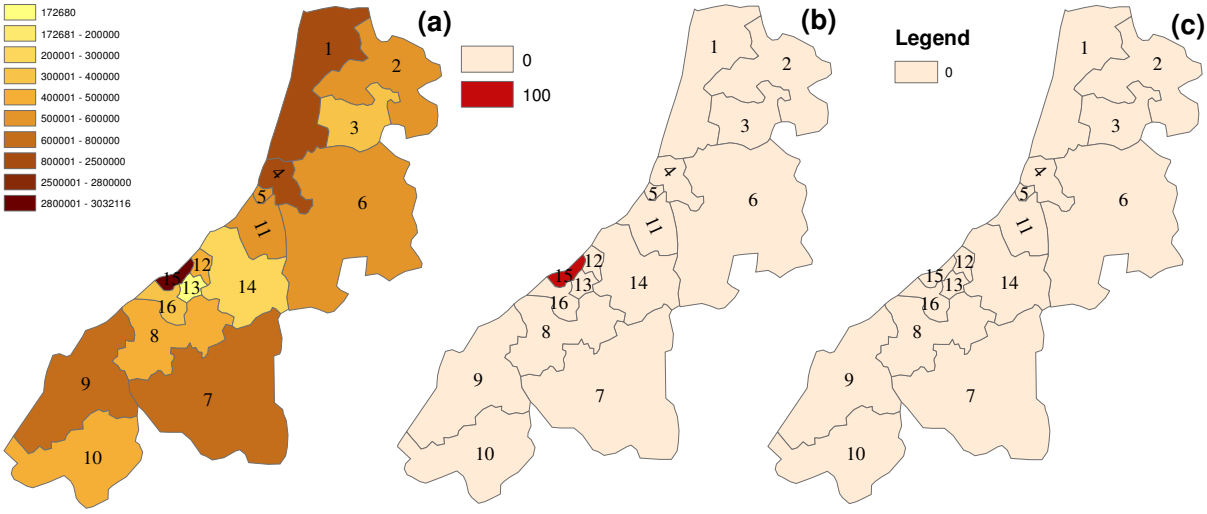

the 16 regions. The region of Casablanca named C_{15} is overcrowded with a population of about 3.5 million of citizens, then the region of Kenitra C_1 with a total population of approximately 1.5 million citizens, then the region of El Jadida C_9 with 1.2 million habitats, then the regions surrounding the metropolis C_{15} with populations which does not exceed 450,000 and the other regions of these two provinces which have an average population of around 700.000 citizens. Fig.2 (b) represents the initial state of the infected individuals in the different regions of the provinces of Casablanca-Settat and Rabat-Sale-Kenitra. It was assumed that only 100 cases of infected in the Casablanca C_{15} region and the other regions not infected yet. In Fig.2 (c) all regions have no recovered populations.

4.4. Scenario 0: Simulation of the multi-region model without any control. In all the rest geographical figures, we consider four time steps (a) $i = 50$, (b) $i = 100$, (c) $i = 150$, and (d) $i = 200$. Dark color represents the highest values. Geographical figures show the transmission of infection between different zones while associated graphs show states' changes over time.

Figures 4.(a), (b), (c) and (d) indicate the number of susceptible people in the 16 regions without any control strategy at the moments $i = 50$, $i = 100$, $i = 150$ and $i = 200$ respectively. We see from Fig. 3 that the number of susceptible people from regions C_7, C_8 and C_{12} are constant until the instant $i = 150$ then decreases by 1.10^5 person. In regions C_2, C_3 and C_{10}

FIGURE 3. Temporal evolution of susceptible populations without the control strategy.

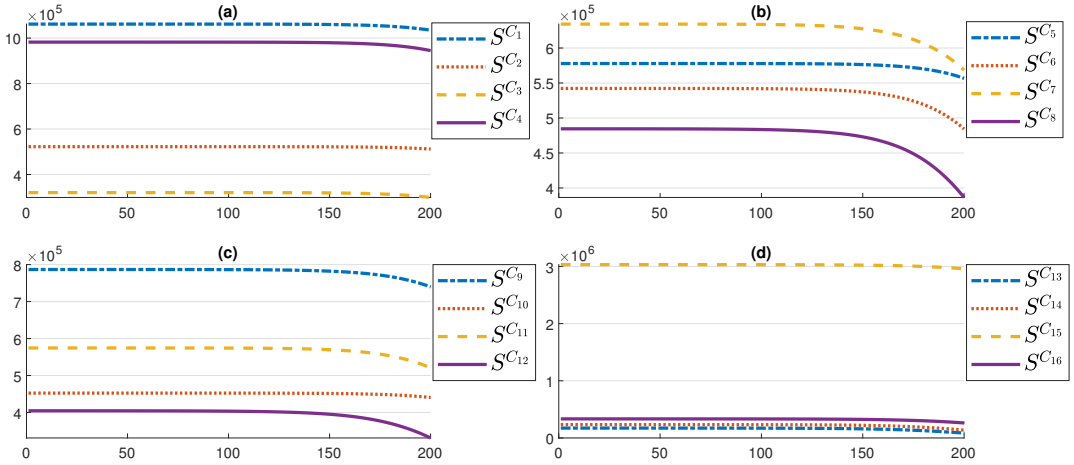

FIGURE 4. Geographical spread of susceptible individuals without the control strategy.

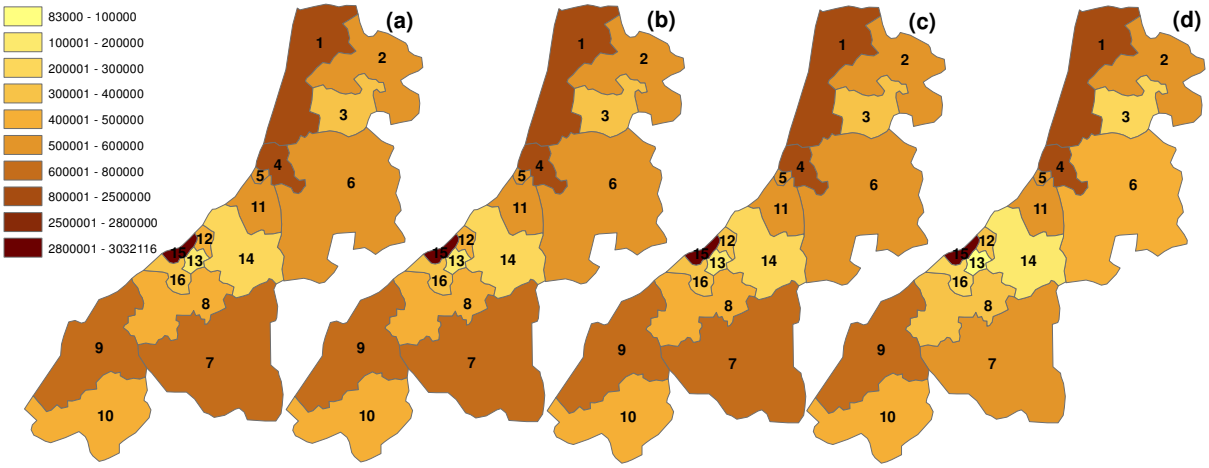

the number of susceptible people is almost constant throughout the period. The other regions experienced a slight decrease from time $i = 150$.

Fig.5 and Fig.6 represent the evolution of the infected without controls in the different regions. We note that at the beginning all the regions did not record any infected except the region C_{15} which recorded 100 infected cases at the start and that from the moment $i = 100$, the number of infected increases exponentially, especially for the regions C_8, C_{13}, C_{14}, which surround the metropolis C_{15}, and which have reached a maximum value of 10^5 infected. The regions C_6, C_7, C_{12}, C_{15}, and C_{16} recorded towards the instant $i = 200$ a maximum value which approaches the value 7.10^4, on the other hand, the regions C_9 and C_{11} reached 5.10^4 infected and the other regions haven't exceeded the number of 3.10^4 cases.

FIGURE 5. Geographical spread of infected individuals without the control strategy.

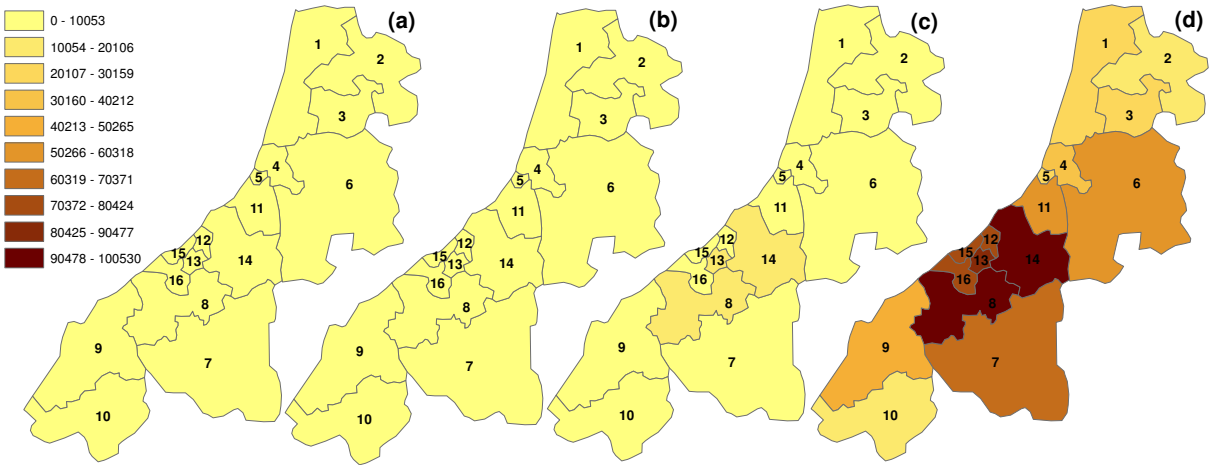

FIGURE 6. Temporal evolution of infected populations without the control strategy.

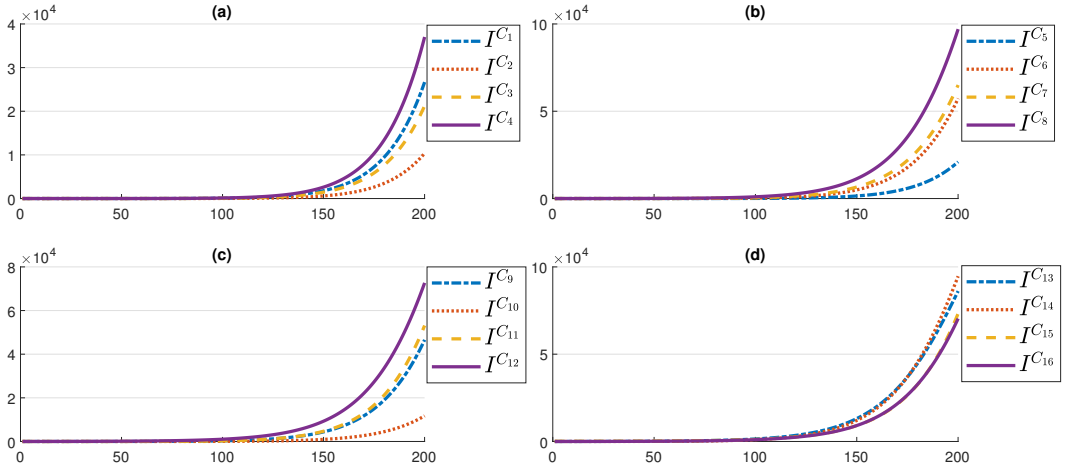

Figures 7 and 8 show the development of recovered without controls in the provinces of Casablanca-Settat and Rabat-Sale-Kenitra. We note that the numbers of the recovered, like the case of the infected, only change from the instant i = 100 and gradually increase to reach for the regions C_8, C_{13} and C_{14}, which surrounds the city of Casablanca, larger values which neighbor the 220 recovered cases, and the regions C_{12}, C_{15} and C_{16} which reached 170 recovered, then the C_6 and C_7 regions which have reached the 130 recovered cases. C_9 and C_{11} reached the end of the period the 100 cases recovered, and in the other regions which are geographically further from C_{15} have do not exceed the 70 cases at the time $i = 200$.

FIGURE 7. Geographical spread of recovered individuals without the control strategy.

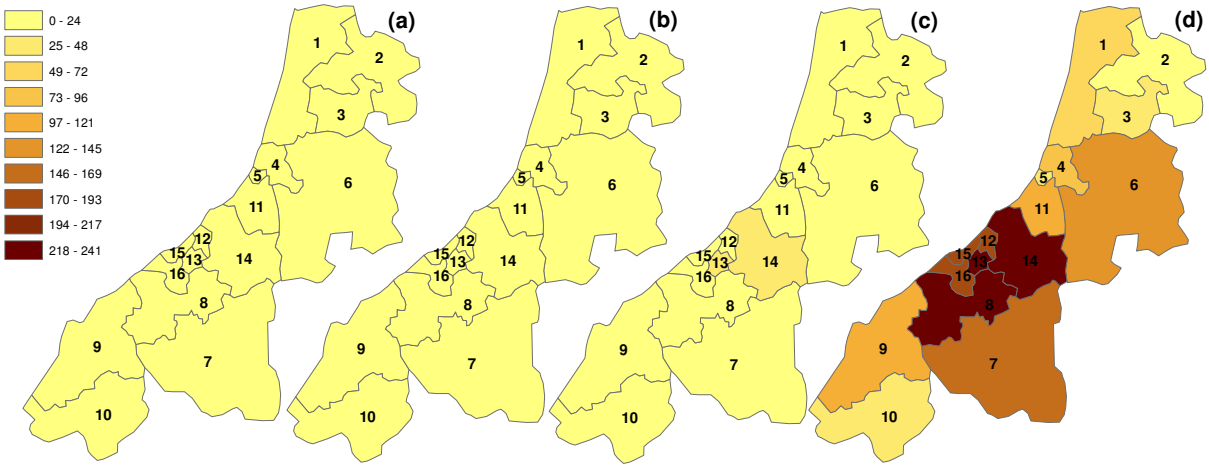

FIGURE 8. Temporal evolution of recovered populations without the control strategy.

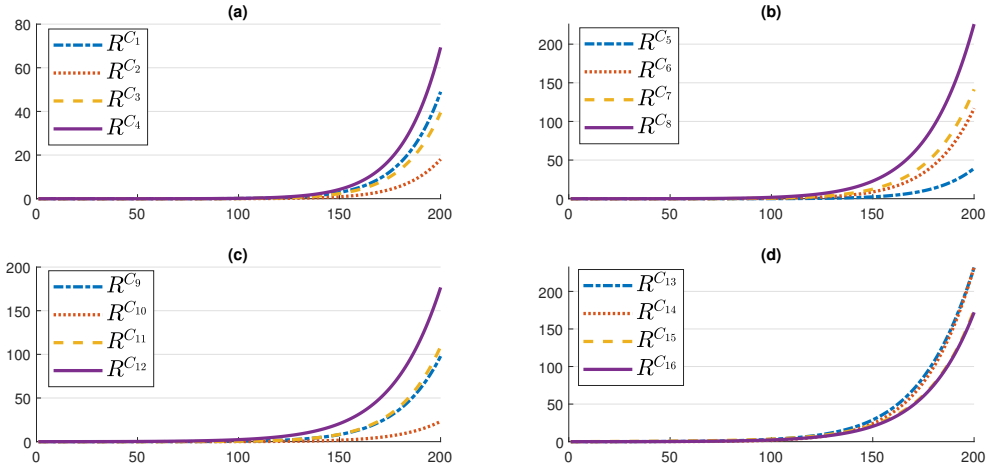

4.5. Scenario 1: Travel-restriction only where $\mathscr{I}^{\mathscr{T}}{}_{min} = 500$. Figures 9 and 10 show the number of susceptible people from the 16 regions applying the travel-restriction control strategy from 500 infected. In all regions, the number of susceptible individuals remains constant throughout the strategy period. On the other hand, for the case without control, the number of susceptible people experienced a slight decrease from the instant $i = 150$ to reach a regression of 10^5 cases towards the end.

Figures 11 and 12 represent the evolution of the infected by applying the travel-restriction control strategy from 500 infected in the different regions. We note that at the beginning all the regions register no infected and that from the instant $i = 100$, the number of infected increases rapidly, especially for the regions C_8, C_{13}, C_{14}, which surround the metropolis C_{15}, and who

FIGURE 9. Temporal evolution of susceptible populations with only the travel-restriction control where $\mathscr{I}^{\mathscr{T}}{}_{min} = 500$.

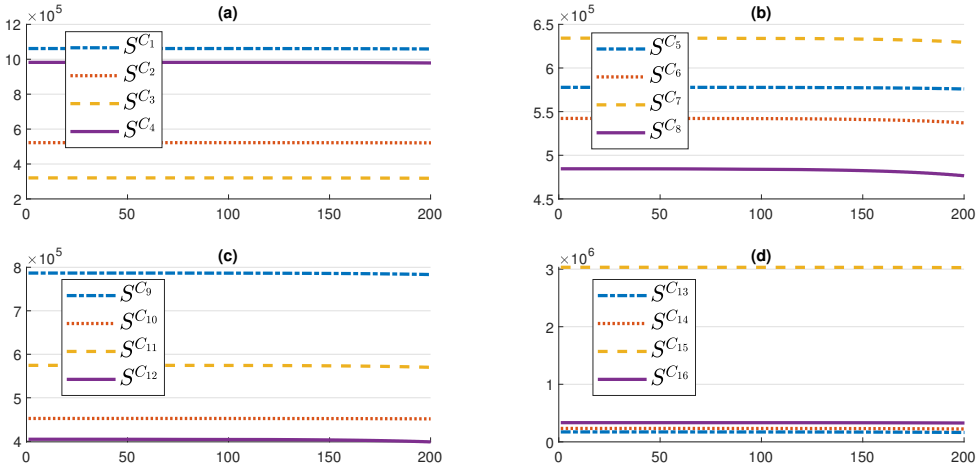

FIGURE 10. Geographical spread of susceptible individuals with only the travel-restriction control where $\mathscr{I}^{\mathscr{T}}{}_{min} = 500$.

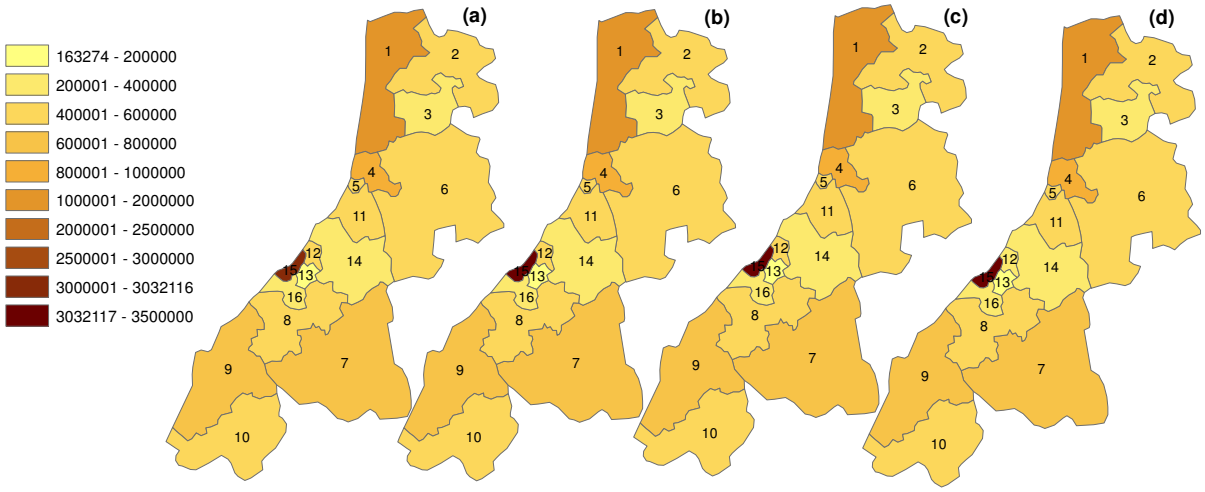

have reached a maximum value of 8000 infected. The regions C_{12}, C_{15}, and C_{16} recorded, at the moment $i = 200$, a maximum value which is close to 6000 cases, then the regions C_6, C_7 and C_{11} reached the 5000 cases, on the other hand, the regions C_1, C_3, C_4, C_5 and C_9 reached values less than 3000 infected and regions C_2 and C_{10} did not exceed the number 1000 cases. On the other hand, without a control strategy, the infected began to evolve from the moment $i = 150$ and recorded numbers of infected 10 times more than with the travel-restriction strategy.

FIGURE 11. Temporal evolution of infected populations with only the travel-restriction control where $\mathscr{J}^{\mathscr{T}}{}_{min} = 500$.

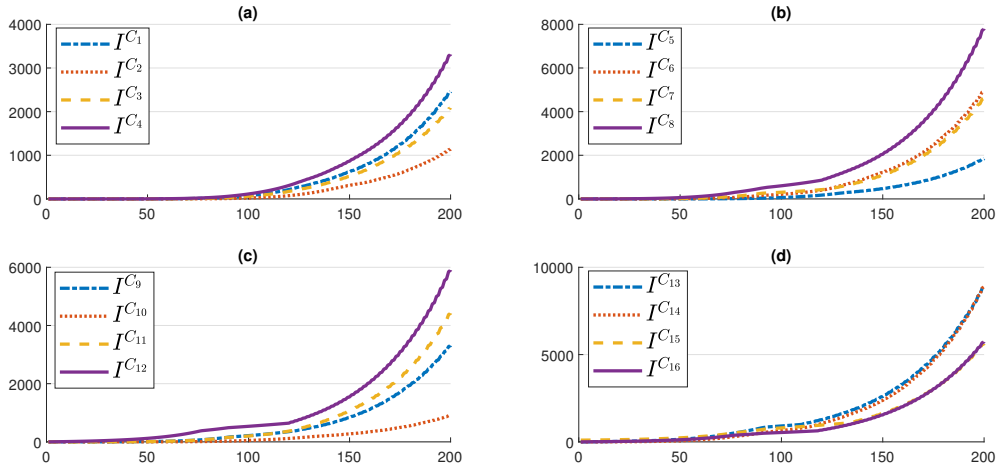

FIGURE 12. Geographical spread of infected individuals with only the travel-restriction control where $\mathscr{J}^{\mathscr{T}}{}_{min} = 500$.

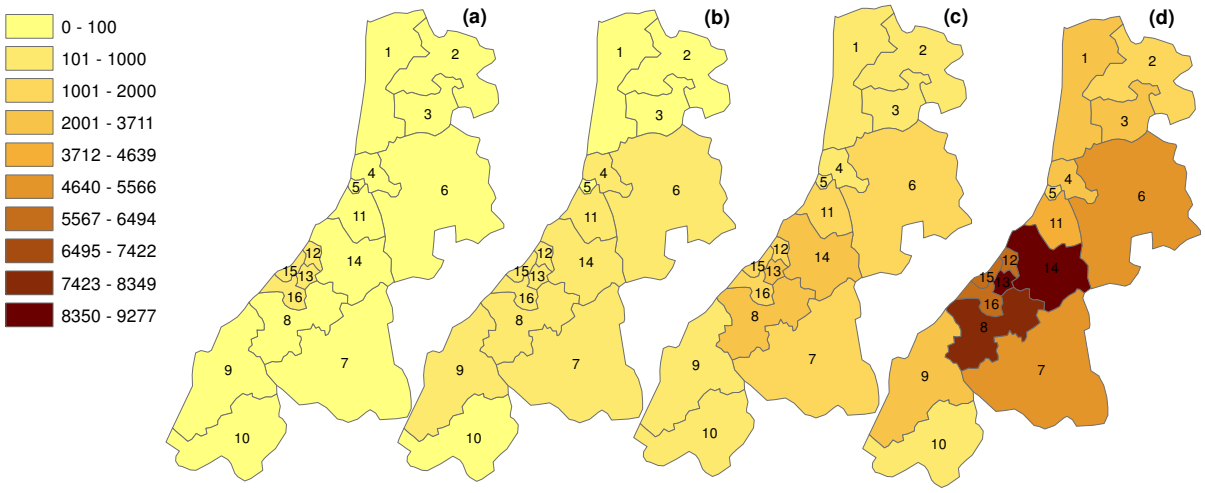

Figures 13 and 14 show the evolution of the recovered with the strategy of travel-restriction controls from 500 infected in the provinces of Casablanca-Settat and Rabat-Sale-Kenitra. It is noted in the regions closest to metropolitan C_{15}, the numbers of recovered persons began to change from the time $i = 70$. Then the other regions further afield, their numbers of recovered only change from the instant $i = 100$ and gradually increase to reach their maximum values at the end of the controls campaign. These numbers of recovered are very low compared to the case without control which does not exceed 30 cases for the regions close to Casablanca and

FIGURE 13. Temporal evolution of recovered populations with only the travel-restriction control where $\mathscr{I}^{\mathscr{T}}{}_{min} = 500$.

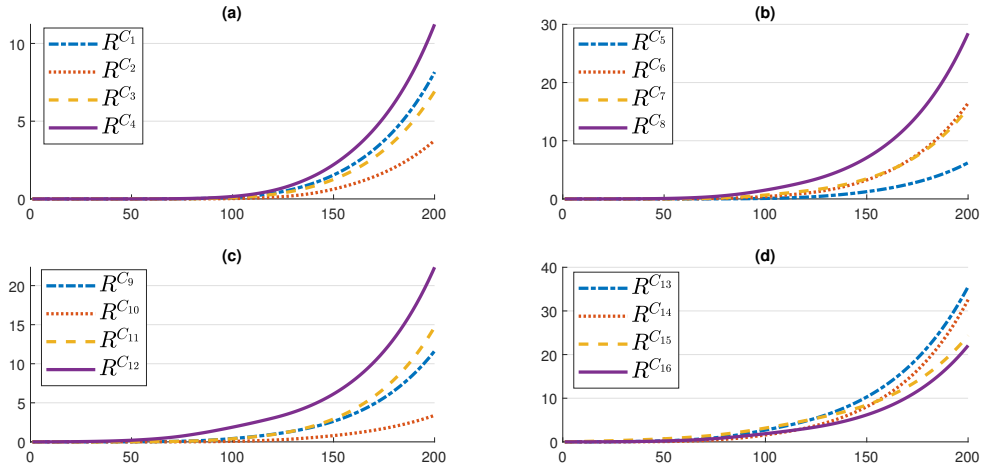

FIGURE 14. Geographical spread of recovered individuals with only the travel-restriction control where $\mathscr{I}^{\mathscr{T}}{}_{min} = 500$.

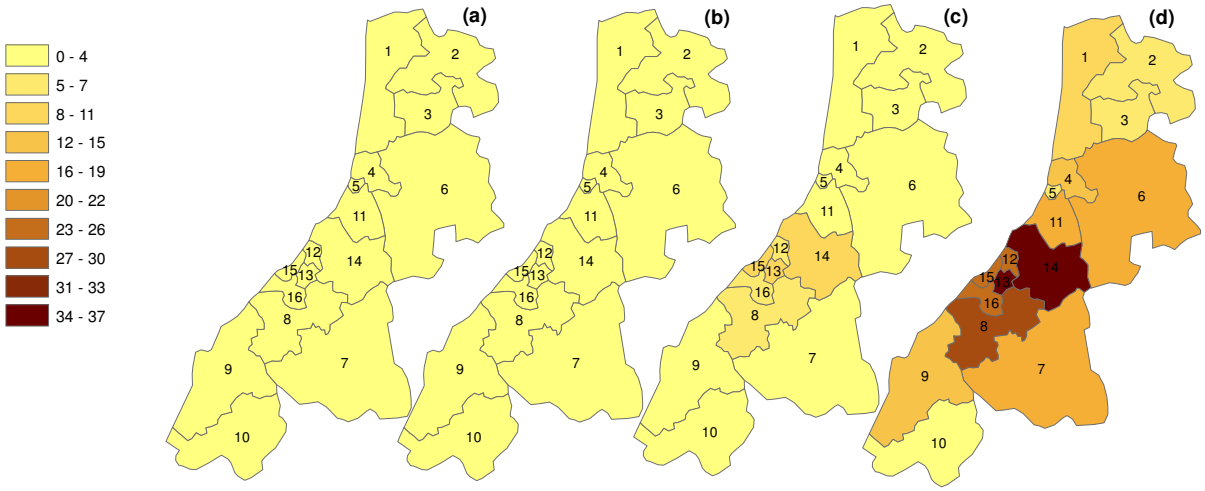

the other regions less than 10 cases and this is due to the fact that the numbers of infected are also low compared to the case without control.

4.6. Scenario 2: Travel-restriction only where $\mathscr{I}^{\mathscr{T}}{}_{min} = 0$. Now, we propose another strategy which consists in defining a travel-restriction on all the provinces from 0 infected i.e by blocking the travel between the regions. This type of strategy is introduced when there is a second wave of the epidemic, when we detect infections in a region and we are aware of the

FIGURE 15. Temporal evolution of susceptible populations with only the travel-restriction control where $\mathscr{I}^{\mathscr{T}}{}_{min} = 0$.

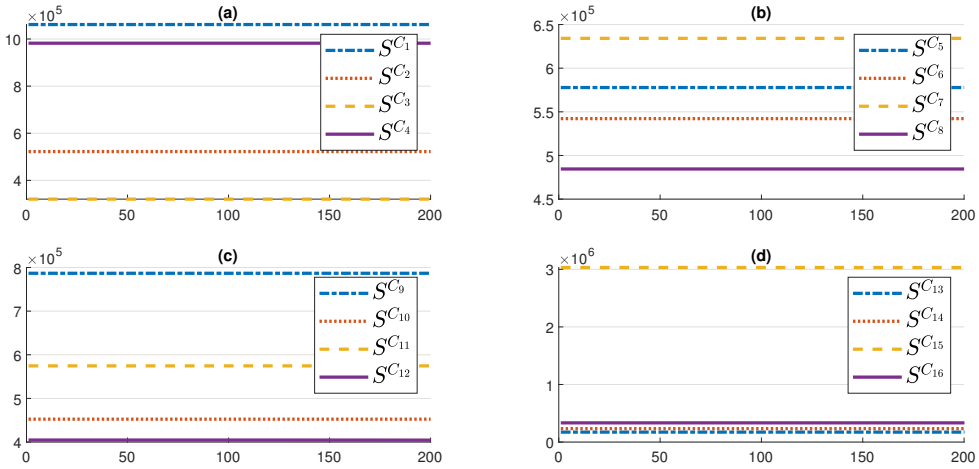

FIGURE 16. Geographical spread of susceptible individuals with only the travel-restriction control where $\mathscr{I}^{\mathscr{T}}{}_{min} = 0$.

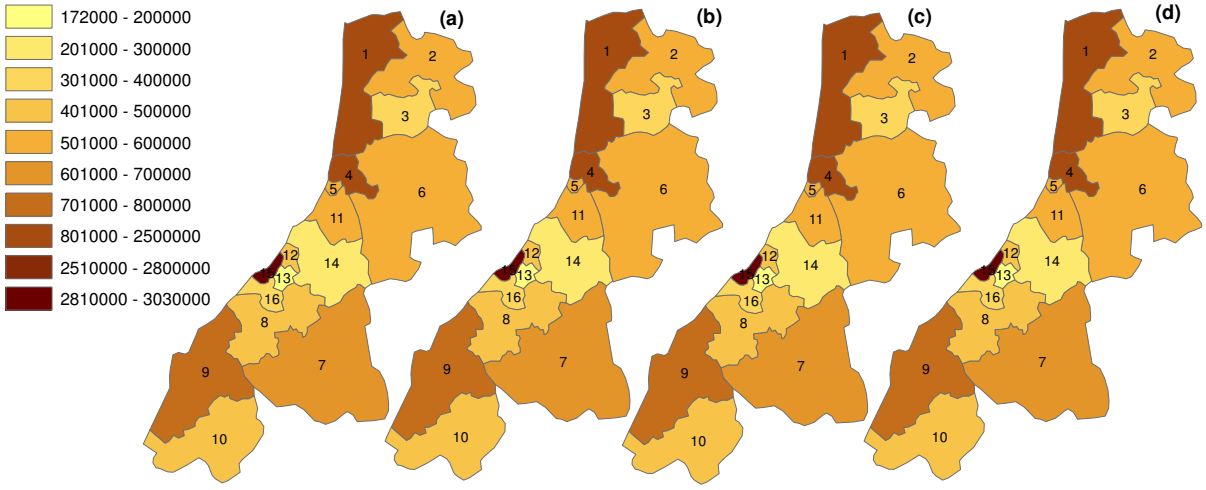

gravity of the virus spread, for example, the case of the Corona-virus pandemics (SARS, MERS, or COVID-19) or Ebola ...

Figures 15 and 16 show the evolution of the numbers of susceptible people in the 16 regions by applying the travel-restriction strategy in all regions from zero infection. We note that throughout the strategy, the number of susceptible remained constant in all 16 regions.

Figures 17 and 18 show the evolution of the numbers of infected in all regions of the provinces of Casablanca-Settat and Rabat-Sale-Kenitra by applying the travel-restriction strategy in all

FIGURE 17. Temporal evolution of infected populations with only the travel-restriction control where $\mathscr{I}^{\mathscr{T}}{}_{min} = 0$.

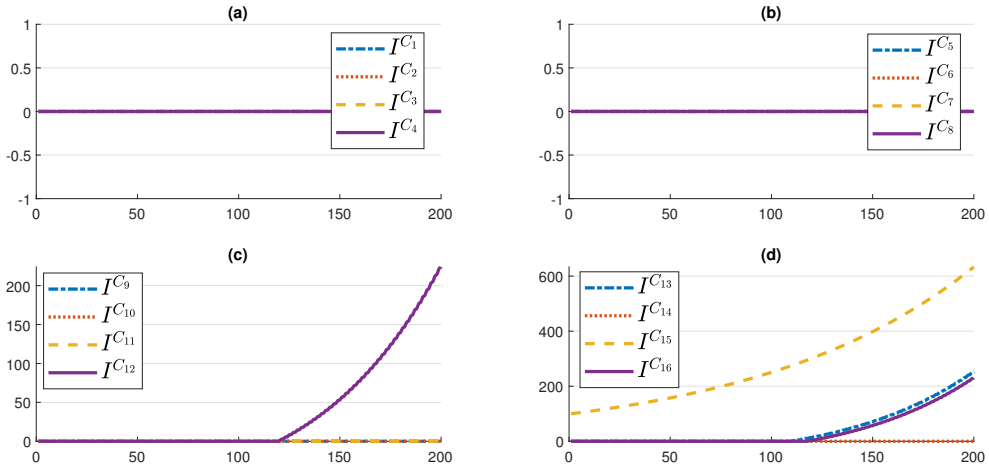

regions, from the appearance of infection in a region and choose blocking trips between regions. In this case, all the regions did not experience any infection throughout the period except the city of Casablanca C_{15} which experienced 100 infected at the initial time and this number increased to reach at the moment $i = 200$, 650 infected. For regions C_{12}, C_{13} and C_{16} only experienced an infection at the time $i = 120$ and from that moment the number of infections increased to reach the maximum number of 250 cases at the end of the period. So the infected are only limited in the regions close to C_{15}, on the other hand without control the infected progress exponentially from the instant $i = 100$ and reach values between 10^4 and 10^5 infected.

Like the numbers of infected with travel-restriction strategy from zero infected, all regions display 0 recovered throughout the period, except region C_{15} which experienced 6 cases of recovered towards the end of the period, as it can be seen from Fig.19 and Fig.20. Since in this strategy the numbers of infected individuals are less important than with the strategy without control.

4.7. Scenario 3: Travel-restriction and vaccination controls where $\mathscr{I}^{\mathscr{T}}{}_{min} = 1000$ and $\mathscr{I}^{\mathscr{V}}{}_{min} = 500$. Figures 21 and 22 show the evolution of susceptible people in the different regions of the provinces of Casablanca-Settat and Rabat-Sale-Kenitra with the application of a vaccination strategy from 500 infected and travel-restriction from 1000 infected. We notice that the susceptible individuals of regions C_8, C_{12}, C_{13}, C_{14}, C_{15} and C_{16} that are closest to

FIGURE 18. Geographical spread of infected individuals with only the travel-restriction control where $\mathscr{J}^{\mathscr{T}}{}_{min} = 0$.

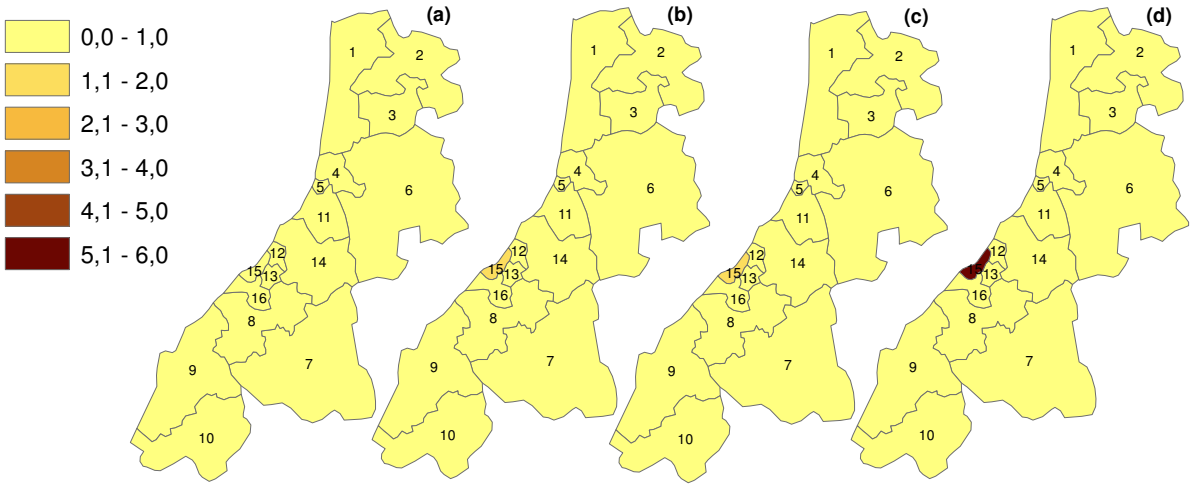

FIGURE 19. Temporal evolution of recovered populations with only the travel-restriction control where $\mathscr{J}^{\mathscr{T}}{}_{min} = 0$.

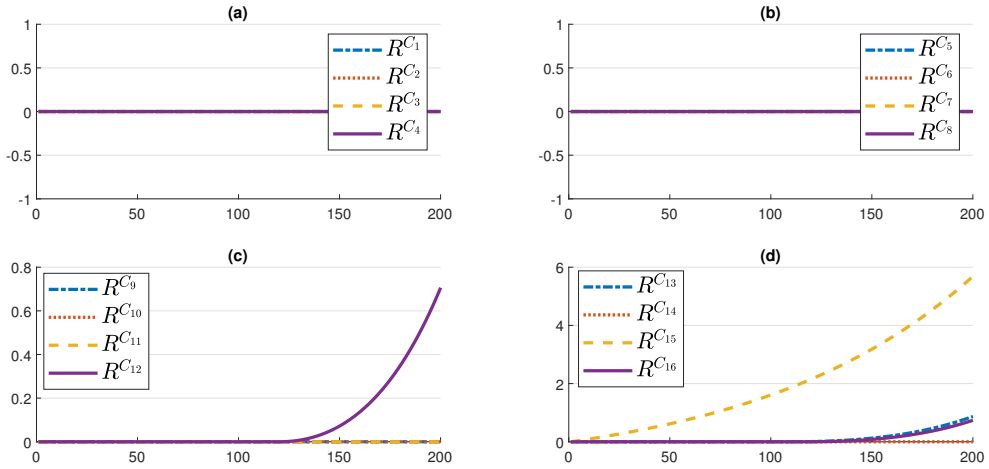

Casablanca begins to decrease very quickly and reach towards 0 from the moment $i = 85$, then the susceptible of regions C_6, C_7, C_9, $_{C11}$ which converges to 0 from the moment $i = 115$ and after those of the most distant regions C_1 and C_4 from Casablanca from $i = 130$ and finally the extreme regions C_2 and C_{10} from the moment $i = 180$. So for this strategy, the numbers of susceptible individuals tend towards 0 from a certain moment, on the other hand for the previous strategies the numbers of susceptibles remain almost constant and decrease slightly from the instant $i = 150$.

FIGURE 20. Geographical spread of recovered individuals with only the travel-restriction control where $\mathscr{I}^{\mathscr{T}}{}_{min} = 0$.

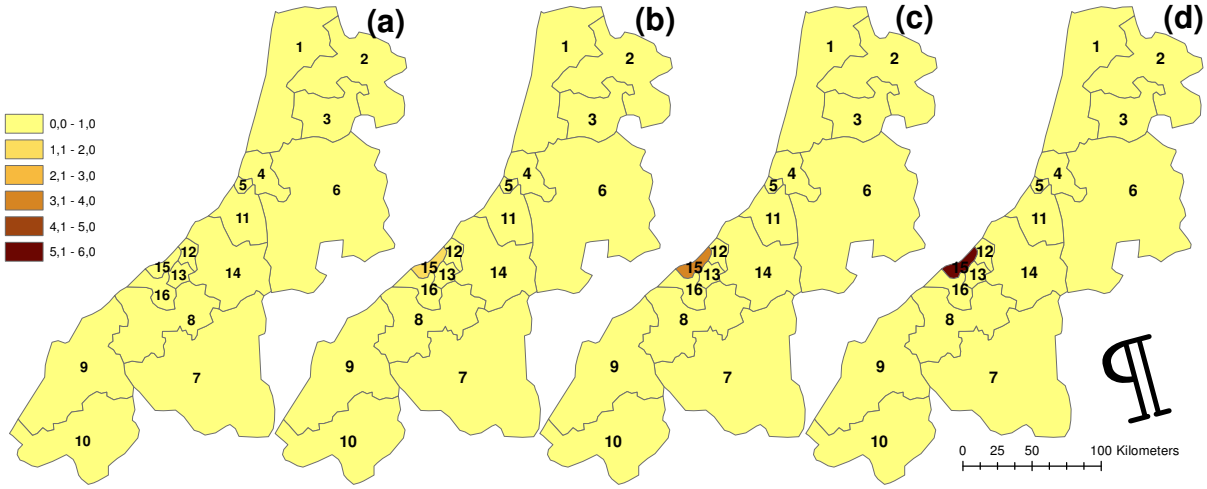

FIGURE 21. Temporal evolution of susceptible populations with the the travel-restriction and vaccination controls where $\mathscr{I}^{\mathscr{T}}{}_{min} = 1000$ and $\mathscr{I}^{\mathscr{V}}{}_{min} = 500$.

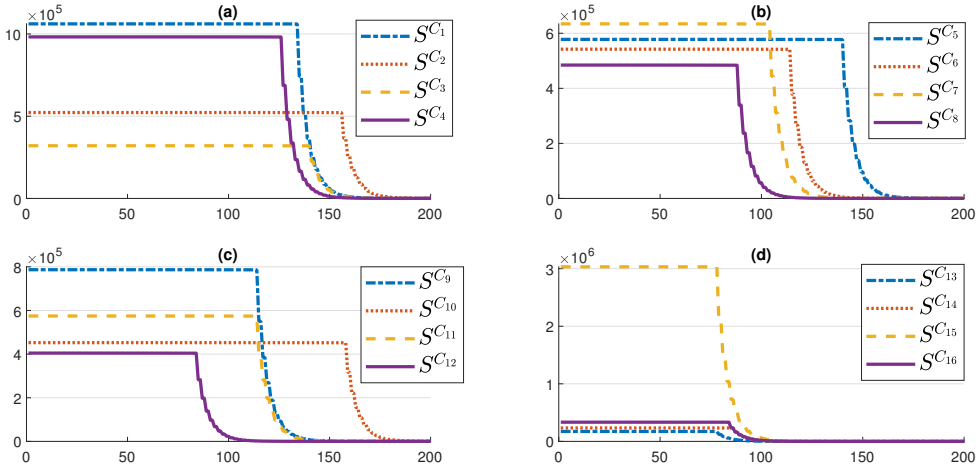

Figures 23 and 24 represent the evolution of the infected in the 16 regions by applying the strategy which combines treatment as soon as the 500 infected appear and travel-restriction from 1000 infected in a region. It is noted that the infected from regions C_8, C_{12}, C_{13}, C_{14}, C_{15} and C_{16} which surround the region of Casablanca, that experienced the appearance of 100 cases infected in the initial state, experienced an increase from the start of the strategy, then the regions C_6, C_7, C_9, C_{11} which started to grow from the time $i = 50$, then the regions farthest from Casablanca which started to grow at the time $i = 75$. All infected from the 16 regions reach

FIGURE 22. Geographical spread of susceptible individuals with the the travel-restriction and vaccination controls where $\mathscr{I}^{\mathscr{T}}{}_{min} = 1000$ and $\mathscr{I}^{\mathscr{V}}{}_{min} = 500$.

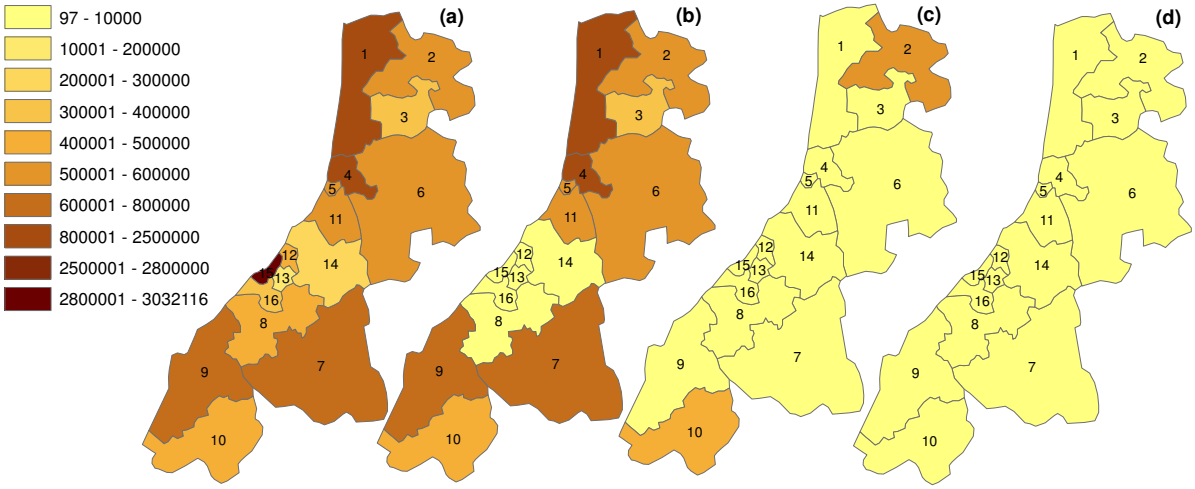

FIGURE 23. Temporal evolution of infected populations with the the travel-restriction and vaccination controls where $\mathscr{I}^{\mathscr{T}}{}_{min} = 1000$ and $\mathscr{I}^{\mathscr{V}}{}_{min} = 500$.

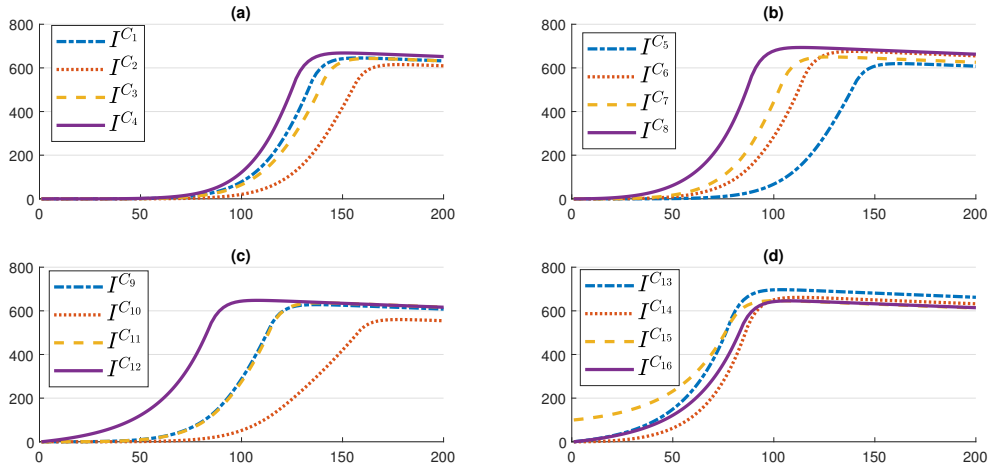

the maximum value of 650 cases infected at the instant $i = 100$ and remain stagnant until the end of the period. With this strategy, the travel-restriction application does not applied since the infected not exceed 1000 cases. On the other hand, this strategy gives good results compared to without control and also compared to the strategy with travel-restriction at 500 infected, but less effective than the strategy with travel-restriction at 0 infected.

Figures 25 and 26 show the evolution of the recovered in the 16 regions by applying the vaccination strategy from 500 infected and the travel-restriction from 1000 infected. It is noted

FIGURE 24. Geographical spread of infected individuals with the the travel-restriction and vaccination controls where $\mathscr{I}^{\mathscr{T}}{}_{min} = 1000$ and $\mathscr{I}^{\mathscr{V}}{}_{min} = 500$.

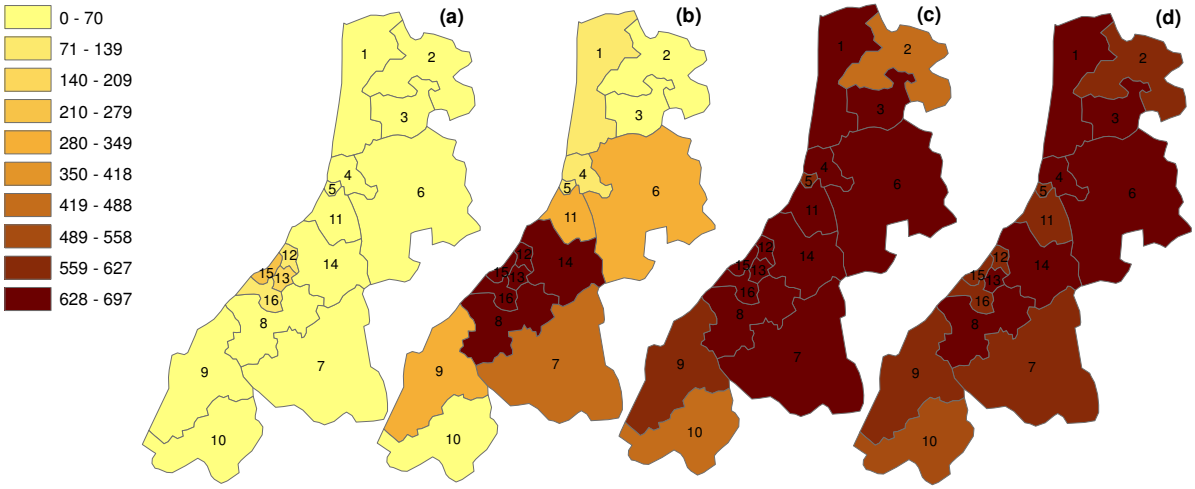

FIGURE 25. Temporal evolution of recovered populations with the the travel-restriction and vaccination controls where $\mathscr{I}^{\mathscr{T}}{}_{min} = 1000$ and $\mathscr{I}^{\mathscr{V}}{}_{min} = 500$.

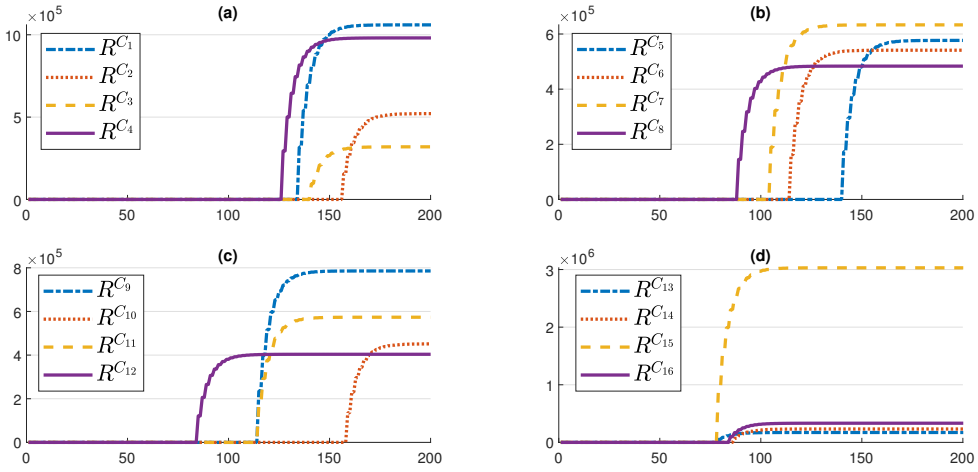

that the numbers of the recovered people of all the regions believe very quickly, starting from the instants $i = 80$, $i = 100$, $i = 130$ and $i = 160$, with maximum values which vary between 3.10^5 and 3.10^6. The regions closest to Casablanca begin to grow at the start, then the least close and then the farthest from Casablanca. This strategy gives better results for the recovered than that without control, whose recovered does not exceed 230 cases, or with the strategies with travel-restriction at 500 infected or at 0 infected that do not exceed the 35 recovered.

FIGURE 26. Geographical spread of recovered individuals with the the travel-restriction and vaccination controls where $\mathscr{I}^{\mathscr{T}}{}_{min} = 1000$ and $\mathscr{I}^{\mathscr{V}}{}_{min} = 500$.

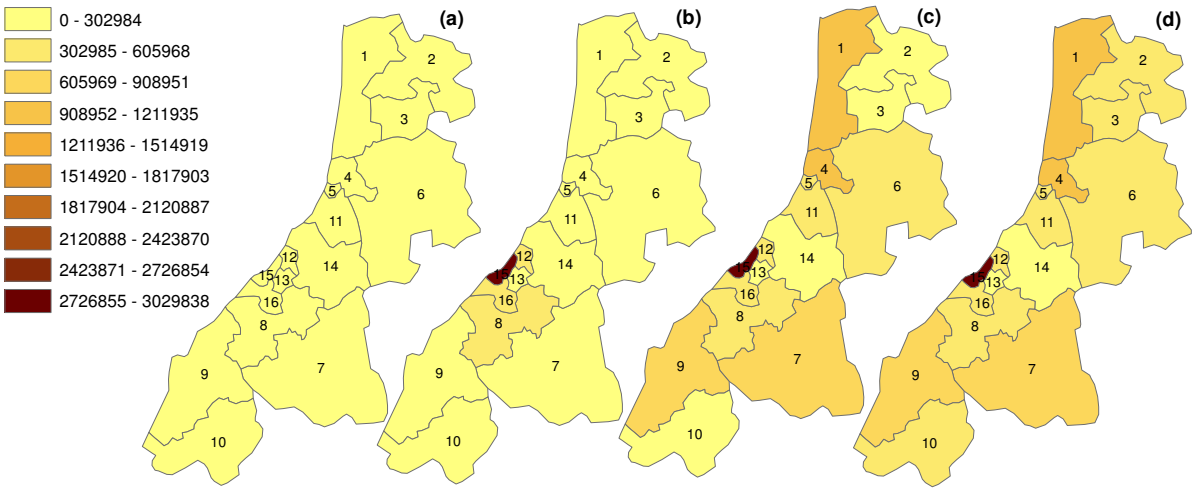

4.8. Scenario 4: Travel-restriction and vaccination controls where $\mathscr{I}^{\mathscr{T}}{}_{min} = 500$ and $\mathscr{I}^{\mathscr{V}}{}_{min} = 500$. Figures 27 and 28 represents the evolution of susceptible people in the different regions of the provinces of Casablanca-Settat and Rabat-Sale-Kenitra with the application of a vaccination strategy from 500 infected and travel-restriction from 500 infected. The evolution of the susceptible is almost the same as that of the strategy with vaccination at 500 infected and travel-restriction at 1000 infected with a slight improvement in convergence time towards 0. We notice that the susceptibles of regions C_8, C_{12}, C_{13}, C_{14}, C_{15} and C_{16} that are closest to Casablanca begins to decrease very quickly and reach towards 0 from the moment $i = 80$, then the susceptible of regions C_6, C_7, C_9, $_{C11}$ which converges to 0 from the moment $i = 100$ and after those of the most distant regions C_1 and C_4 from Casablanca from $i = 125$ and finally the extreme regions C_2, C_5 and C_{10} from the moment $i = 150$. So for this strategy, the numbers of susceptible individuals tend towards 0 from a certain moment, on the other hand for the previous strategies the numbers of susceptible population remain almost constant and decrease slightly from the instant $i = 150$.

Figures 29 and 30 represent the evolution of the infected in the 16 regions by applying the strategy which combines treatment as soon as the 500 infected appear and travel-restriction from 500 infected in a region. With this strategy, the numbers of infected also remain stagnant from the moment $i = 100$ and do not exceed the value of 600 cases in almost all regions and

FIGURE 27. Temporal evolution of susceptible populations with the the travel-restriction and vaccination controls where $\mathscr{I}^{\mathscr{T}}{}_{min} = 500$ and $\mathscr{I}^{\mathscr{V}}{}_{min} = 500$.

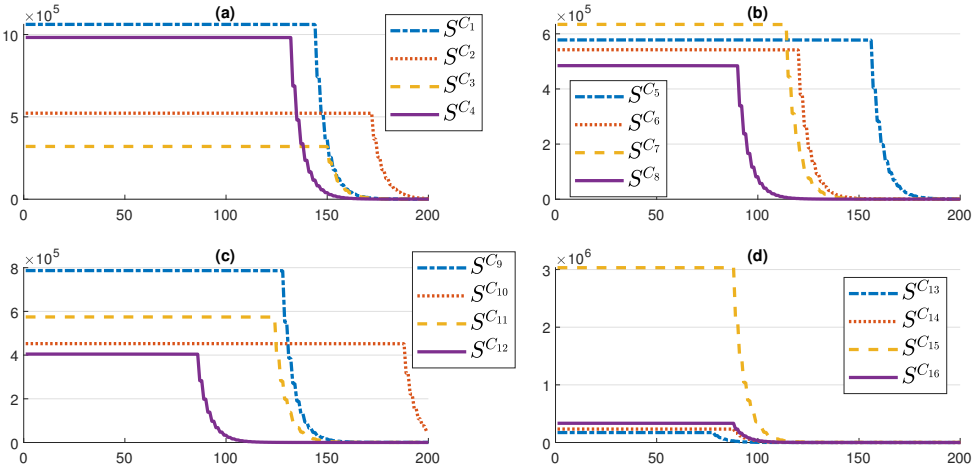

FIGURE 28. Geographical spread of susceptible individuals with the the travel-restriction and vaccination controls where $\mathscr{I}^{\mathscr{T}}{}_{min} = 500$ and $\mathscr{I}^{\mathscr{V}}{}_{min} = 500$.

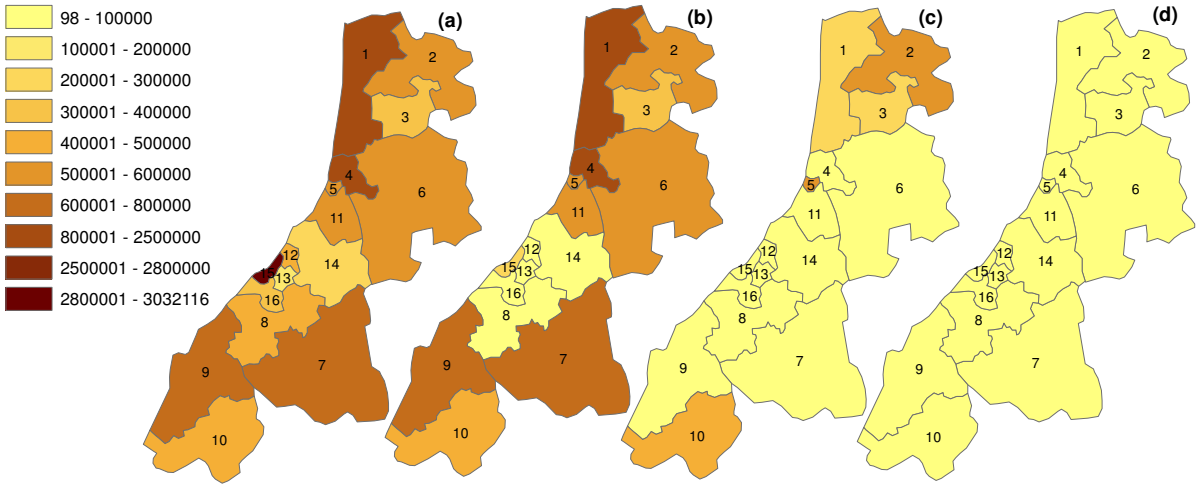

remain stagnant until the end of the period. We notice a slight improvement compared to the vaccination strategy for 500 infected and travel-restriction for 1000 infected and we can say that it gives almost the same values. It is noted that the infected from regions C_8, C_{12}, C_{13}, C_{14}, C_{15} and C_{16} which surround the city of Casablanca, that experienced the appearance of 100 cases infected in the initial state, experienced an increase from the start of the strategy, then the regions C_6, C_7, C_9, C_{11} which started to grow from the time $i = 50$, then the regions farthest from Casablanca which started to grow at the time $i = 75$. On the other hand, this strategy gives good

FIGURE 29. Temporal evolution of infected populations with the the travel-restriction and vaccination controls where $\mathscr{I}^{\mathscr{T}}{}_{min} = 500$ and $\mathscr{I}^{\mathscr{V}}{}_{min} = 500$.

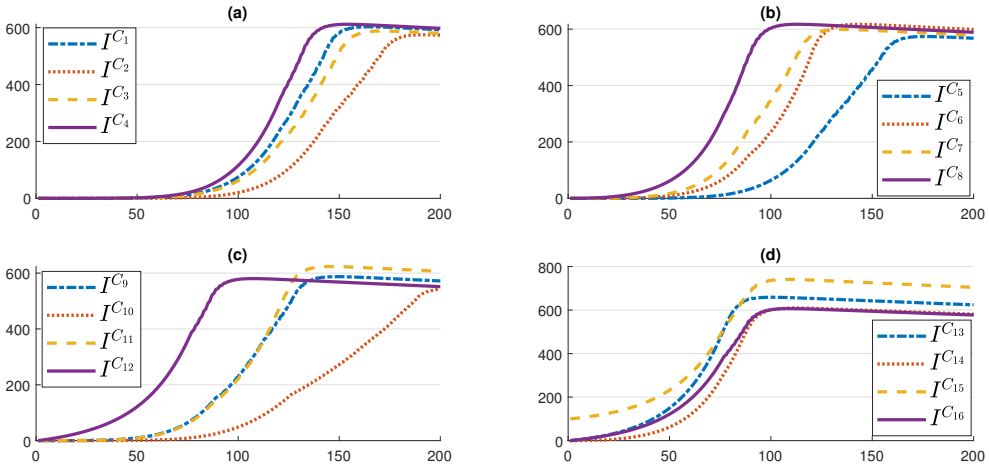

FIGURE 30. Geographical spread of infected individuals with the the travel-restriction and vaccination controls where $\mathscr{I}^{\mathscr{T}}{}_{min} = 500$ and $\mathscr{I}^{\mathscr{V}}{}_{min} = 500$.

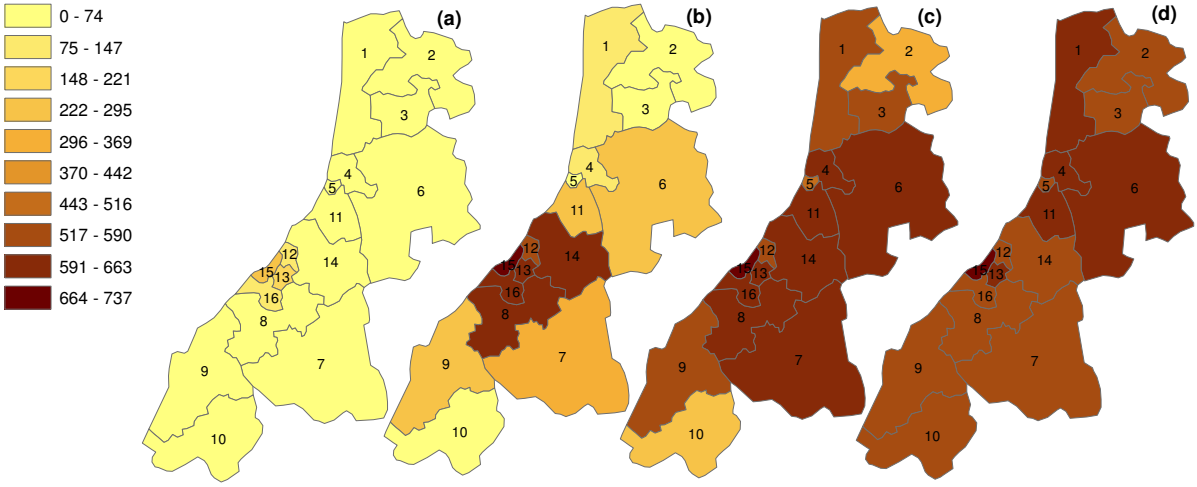

results compared to without control and also compared to the strategy with travel-restriction at 500 infected, but less effective than the strategy with travel-restriction at 0 infected.

Figures 31 and 32 show the evolution of the recovered in the 16 regions by applying the vaccination strategy from 500 infected and the travel-restriction from 500 infected. We notice a slight improvement compared to the vaccination strategy for 500 infected and travel-restriction for 1000 infected. It is noted that the numbers of the recovered people of all the regions believe very quickly, starting from the instants $i = 80$, $i = 130$, $i = 160$ and $i = 180$, with maximum

FIGURE 31. Temporal evolution of recovered populations with the the travel-restriction and vaccination controls where $\mathscr{I}^{\mathscr{T}}{}_{min} = 500$ and $\mathscr{I}^{\mathscr{V}}{}_{min} = 500$.

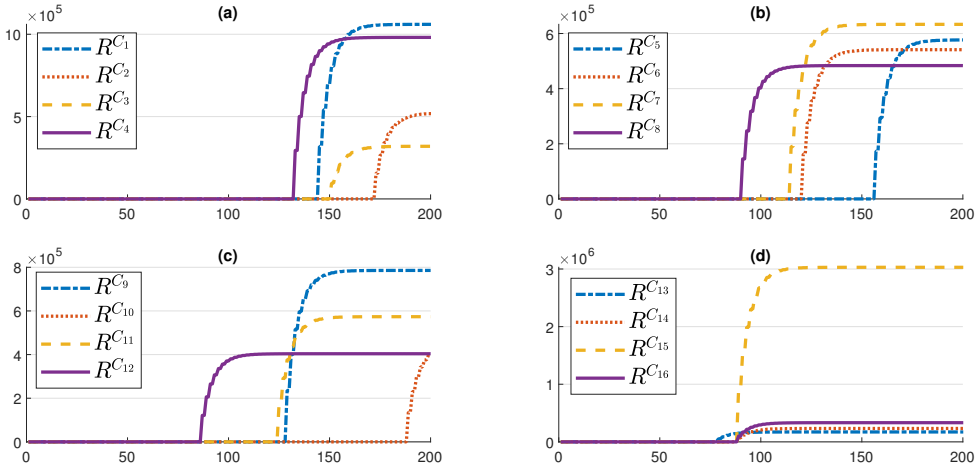

FIGURE 32. Geographical spread of recovered individuals with the the travel-restriction and vaccination controls where $\mathscr{I}^{\mathscr{T}}{}_{min} = 500$ and $\mathscr{I}^{\mathscr{V}}{}_{min} = 500$.

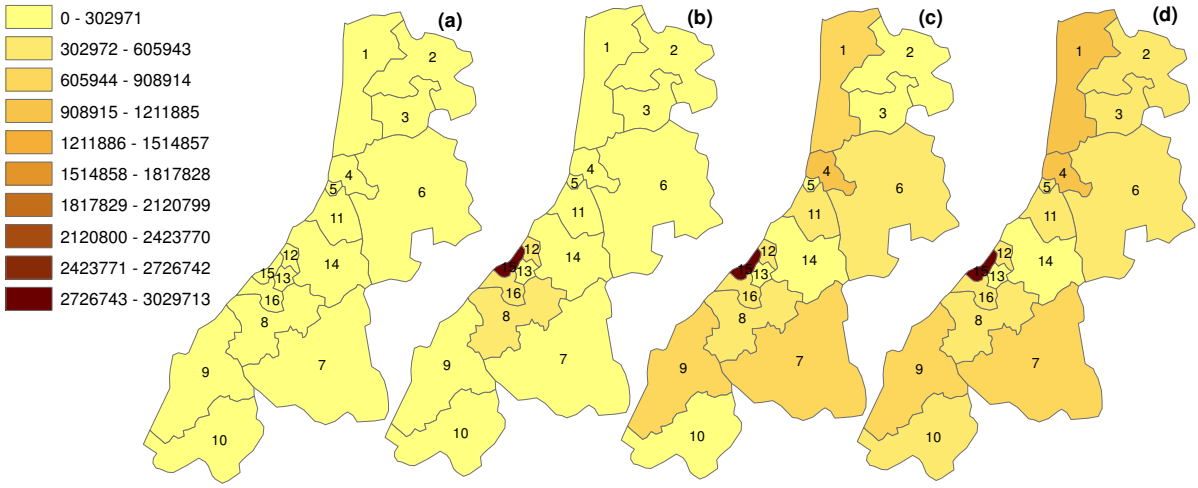

values which vary between 3.10^5 and 3.10^6. The regions closest to Casablanca begin to grow at the start, then the least close and then the farthest from Casablanca. This strategy gives better results for the recovered than that without control, whose recovered does not exceed 230 cases, or with the strategies with travel-restriction at 500 infected or at 0 infected that do not exceed the 35 recovered.

FIGURE 33. Temporal evolution of susceptible populations with the the travel-restriction and vaccination controls where $\mathscr{I}^{\mathscr{T}}{}_{min} = 0$ and $\mathscr{I}^{\mathscr{V}}{}_{min} = 500$.

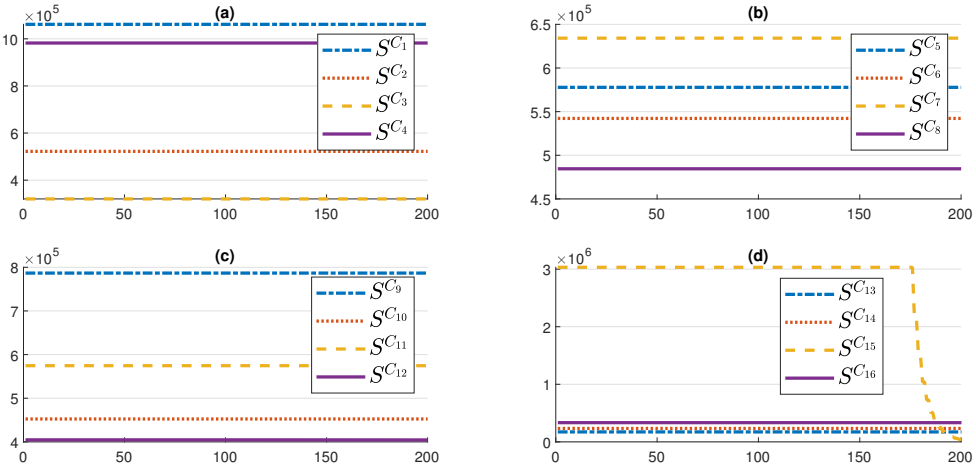

FIGURE 34. Geographical spread of susceptible individuals with the the travel-restriction and vaccination controls where $\mathscr{I}^{\mathscr{T}}{}_{min} = 0$ and $\mathscr{I}^{\mathscr{V}}{}_{min} = 500$.

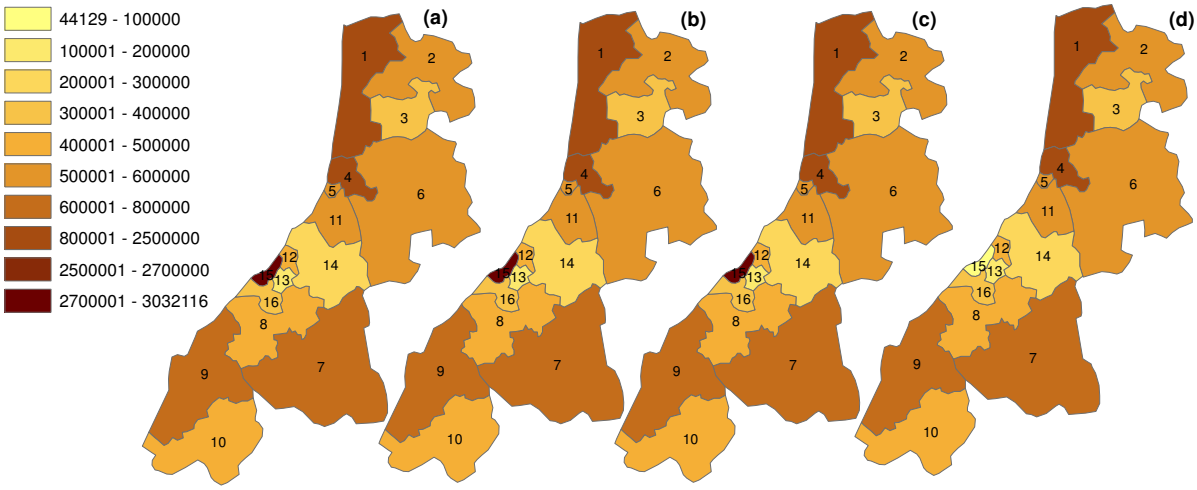

4.9. Scenario 5: Travel-restriction and vaccination controls where $\mathscr{I}^{\mathscr{T}}{}_{min} = 0$ and $\mathscr{I}^{\mathscr{V}}{}_{min} = 500$. Figures 33 and 34 show the evolution of the numbers of susceptible people in the 16 regions by applying the vaccination strategy from 500 infected and the travel-restriction strategy in all regions from zero infection. We note that throughout the strategy, the number of susceptible remained constant in all 16 regions, except for the region of Casablanca where the susceptible remains stagnant until the moment $i = 180$ then decreases very quickly to reach the value 0 towards the end of the period.

FIGURE 35. Temporal evolution of infected populations with the the travel-restriction and vaccination controls where $\mathscr{I}^{\mathscr{T}}{}_{min} = 0$ and $\mathscr{I}^{\mathscr{V}}{}_{min} = 500$.

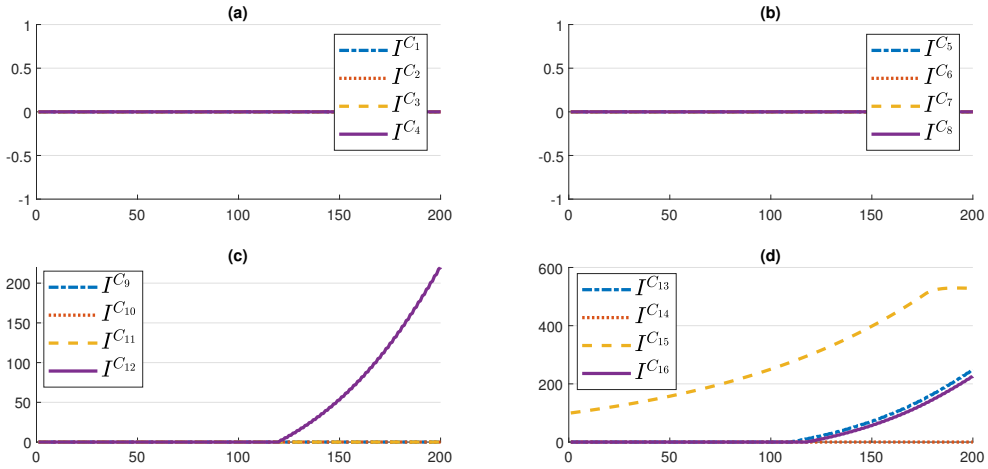

Figures 35 and 36 show the evolution of the numbers of infected in all regions of the provinces of Casablanca-Settat and Rabat-Sale-Kenitra by applying the vaccination strategy from 500 infected and the travel-restriction strategy in all regions from 0 infected. In this case, all the regions did not experience any infection throughout the period except the city of Casablanca C_{15} which experienced 100 infected at the initial time and this number increased to reach at the moment $i = 200$, 520 infected. For regions C_{12}, C_{13} and C_{16} only experienced an infection at the time $i = 120$ and from that moment the number of infections increased to reach the maximum number of 230 cases at the end of the period. So the infected are only limited in the regions close to C_{15}. This strategy gives almost the same results as with the strategy of travel-restriction at 0 infected only, so we can say that this strategy is best compared to the other strategies.

In figure 37 and 38 and like for the numbers of infected with travel-restriction strategy from zero infected, all regions display 0 recovered throughout all the period, except region C_{15} which grows from the instant $i = 175$ and reaches its maximum value of 3.10^6 recovered towards the end of the period.

It can be concluded that without a control strategy, the infected explodes and reach extreme values which exceed in almost all regions 4.10^5 infected. With the travel-restriction strategy from 500 infected, the number of infected individuals increase in all regions and vary between 2000 and 8000 cases. So there is a decrease compared to cases when there are no controls.

FIGURE 36. Geographical spread of infected individuals with the the travel-restriction and vaccination controls where $\mathscr{I}^{\mathscr{T}}{}_{min} = 0$ and $\mathscr{I}^{\mathscr{V}}{}_{min} = 500$.

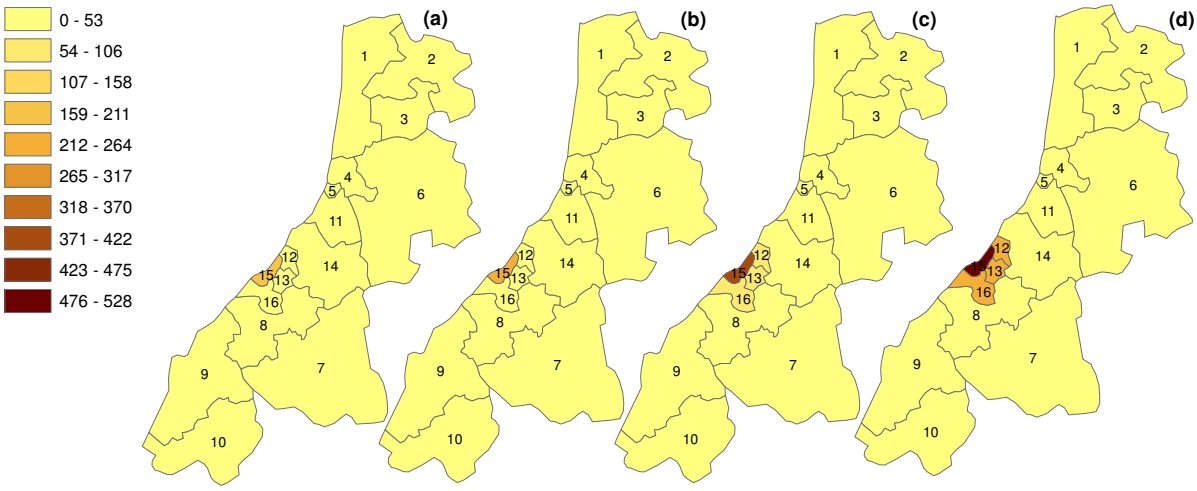

FIGURE 37. Temporal evolution of recovered populations with the the travel-restriction and vaccination controls where $\mathscr{I}^{\mathscr{T}}{}_{min} = 0$ and $\mathscr{I}^{\mathscr{V}}{}_{min} = 500$.

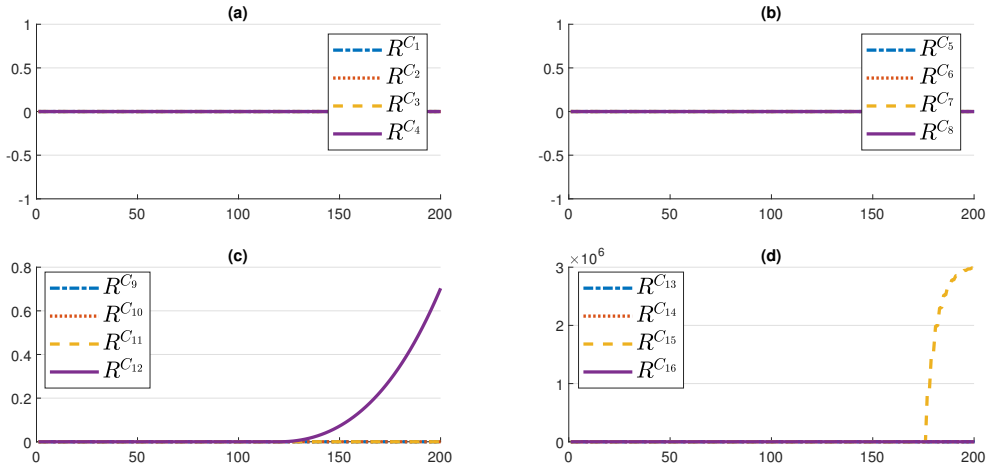

With travel-restriction from 0 infected, the numbers of infected remained almost zero in all regions except the regions closest to Casablanca city that they had maximum values which did not exceed 230 infected and 650 cases in the region C_{15}. So with this strategy, the infections are bounded and limited to the regions which surround the metropolitan area C_{15}. On the other hand, with the vaccination strategy from 500 infections and travel-restriction from 1000 infected individuals, the numbers of infections remain constant with values that do not exceed 650 cases from the moment $i = 100$. With the vaccination strategy from 500 infection and

FIGURE 38. Temporal evolution of recovered individuals with the the travel-restriction and vaccination controls where $\mathscr{I}^{\mathscr{T}}{}_{min} = 0$ and $\mathscr{I}^{\mathscr{V}}{}_{min} = 500$.

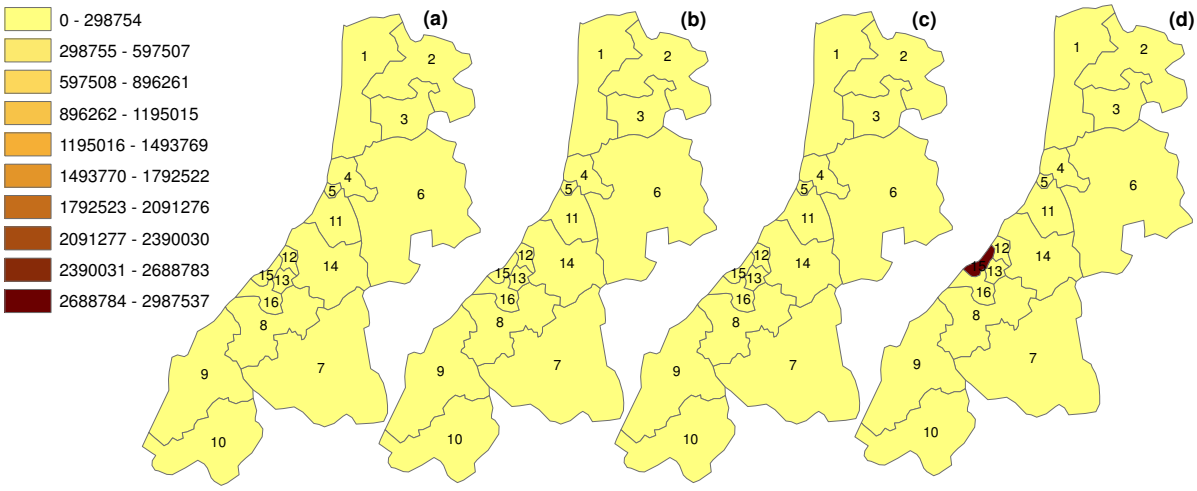

travel-restriction from 500 infection, the numbers of infected individuals also remain stagnant from the moment $i = 100$ and do not exceed the value of 600 cases in almost all regions. We notice a slight improvement compared to the vaccination strategy started from 500 infected and travel-restriction from 1000 infected and we can say that it gives almost the same values. The strategy of vaccination from 500 infected and travel-restriction at 0 infected gives almost the same results as with the strategy of travel-restriction at 0 infected only, with a decrease in infected cases which does not exceed 500 cases in region C_{15} and 230 cases in regions C_{12}, C_{13} and C_{16}, and 0 infected in the other regions. So we can say that this strategy is best compared to the other strategies.

5. CONCLUSION

In this paper, we devised a novel optimization approach that represents a general form of optimal control approaches studied in multi-region framework. We applied this approach to a multi-region discrete epidemic model which has been firstly proposed in [13]. We suggested in this article, a new analysis of infection dynamics in M regions which we supposed to be accessible for health authorities. By defining new importance functions to identify affected areas that must be dealt with, we investigated the effectiveness of optimal vaccination and travel-restriction control approaches, we introduced into the model, control functions associated with appropriate control strategies followed in the targeted regions by mass vaccination campaigns

and restrictions and considering different scenarios to compare different strategies. Based on our numerical simulations, we showed the geographical spread of the epidemic and the influence of each region on another and then we deduced the effectiveness of each strategy followed. We concluded that the last scenario of optimal control approach when ${\mathscr{I}^{\mathscr{T}}}_{min} = 0$ and ${\mathscr{I}^{\mathscr{V}}}_{min} = 500$ has given better results than the other cases regarding the maximization of the number of recovered individuals and minimization of the spread of infection in all regions studied.

DATA AVAILABILITY

Data of the actual populations of the Casablanca-Settat region from [40] and for the Rabat-Salé-Kénitra region from [41].

FUNDING STATEMENT

The author(s) received no financial support for the research, authorship, and/or publication of this article.

CONFLICT OF INTERESTS

The author(s) declare that there is no conflict of interests.

REFERENCES

[1] J. D. Murray, Mathematical biology: I. An Introduction. Interdisciplinary Applied Mathematics, Springer, New York, 2002.

[2] V. Capasso, Mathematical structures of epidemic systems, Lecture Notes in Biomathematics, New York, 1983.

[3] M. Lhous, O. Zakary, M. Rachik, E. M. Magri, A. Tridane, Optimal containment control strategy of the second phase of the covid-19 lockdown in morocco, Appl. Sci. 10 (21) (2020), 7559.

[4] G. F. Medley, N. A. Lindop, W. J. Edmunds, D. J. Nokes, Hepatitis-b virus endemicity: heterogeneity, catastrophic dynamics and control, Nat. Med. 7 (5) (2001), 619–624.

[5] S. A. Bozzette, R. Boer, V. Bhatnagar, J. L. Brower, E. B. Keeler, S. C. Morton, M. A. Stoto, A model for a smallpox-vaccination policy, N. Engl. J. Med. 348 (5) (2003), 416–425.

[6] S. M. Blower, T. Chou, Modeling the emergence of the'hot zones': tuberculosis and the amplification dynamics of drug resistance, Nat. Med. 10 (10) (2004), 1111–1116.

[7] Y.-H. Hsieh, Y.-S. Cheng, Real-time forecast of multiphase outbreak, Emerg. Infect. Dis. 12 (1) (2006), 122.

[8] S. Basu, J. R. Andrews, E. M. Poolman, et al. Prevention of nosocomial transmission of extensively drug-resistant tuberculosis in rural south african district hospitals: an epidemiological modelling study, Lancet 370 (9597) (2007), 1500–1507.

[9] O. Zakary, S. Bidah, M. Rachik, The impact of staying at home on controlling the spread of covid-19: Strategy of control, Mexican J. Biomed. Eng. 42 (1) (2020), 10–26.

[10] B. Sara, Z. Omar, T. Abdessamad, R. Mostafa, F. Hanane, Parameters' estimation, sensitivity analysis and model uncertainty for an influenza a mathematical model: case of morocco, Commun. Math. Biol. Neurosci. 2020 (2020), 57.

[11] O. Zakary, S. Bidah, M. Rachik, H. Ferjouchia, Mathematical model to estimate and predict the covid-19 infections in morocco: Optimal control strategy, J. Appl. Math. 2020 (2020), 9813926.

[12] F. El Kihal, M. Rachik, O. Zakary, I. Elmouki, A multi-regions seirs discrete epidemic model with a travel-blocking vicinity optimal control approach on cells, Int. J. Adv. Appl. Math. Mech. 4 (3) (2017), 60–71.

[13] O. Zakary, M. Rachik, I. Elmouki, On the analysis of a multi-regions discrete sir epidemic model: an optimal control approach, Int. J. Dyn. Control. 5 (3) (2017), 917–930.

[14] O. Zakary, M. Rachik, I. Elmouki, A multi-regional epidemic model for controlling the spread of ebola: awareness, treatment, and travel-blocking optimal control approaches, Math. Meth. Appl. Sci. 40 (4) (2017), 1265–1279.

[15] O. Zakary, M. Rachik, I. Elmouki, A new analysis of infection dynamics: multi-regions discrete epidemic model with an extended optimal control approach, Int. J. Dyn. Control. 5 (4) (2017), 1010–1019.

[16] S. Bidah, O. Zakary, M. Rachik, Stability and global sensitivity analysis for an agree-disagree model: Partial rank correlation coefficient and latin hypercube sampling methods, Int. J. Differ. Equ. 2020 (2020), 5051248.

[17] B. Hamza, B. Sara, Z. Omar, A. Imane, R. Mostafa, New automated optimal vaccination control with a multi-region sirs epidemic mode, Commun. Math. Biol. Neurosci. 2020 (2020), 70.

[18] Z. Rachik, H. Boutayeb, S. Bidah, O. Zakary, M. Rachik, Control of information dissemination in online environments: optimal feedback control, Commun. Math. Biol. Neurosci. 2020 (2020), 86.

[19] Z. Rachik, S. Bidah, H. Boutayeb, O. Zakary, M. Rachik, Understanding the different objectives of information and their mutual impact: multi-information model, Commun. Math. Biol. Neurosci. 2021 (2021), 1.

[20] S. Bidah, O. Zakary, M. Rachik, H. Ferjouchia, Mathematical modeling of public opinions: Parameter estimation, sensitivity analysis, and model uncertainty using an agree-disagree opinion model, Abstr. Appl. Anal. 2020 (2020), 1837364.

[21] G. Zaman, Y. H. Kang, I. H. Jung, Stability analysis and optimal vaccination of an sir epidemic model, BioSystems. 93 (3) (2008), 240–249.

[22] O. Zakary, A. Larrache, M. Rachik, I. Elmouki, Effect of awareness programs and travel-blocking operations in the control of hiv/aids outbreaks: a multi-domains sir model, Adv. Differ. Equ. 2016 (2016), 169.

[23] O. Zakary, M. Rachik, I. Elmouki, On the impact of awareness programs in hiv/aids prevention: an sir model with optimal control, Int. J. Comput. Appl. 133 (9) (2016), 1–6.

[24] M. Roshanfekr, M. H. Farahi, R. Rahbarian, A different approach of optimal control on an hiv immunology model, Ain Shams Eng. J. 5 (1) (2014), 213–219.

[25] Y. Zhou, Y. Liang, J. Wu, An optimal strategy for hiv multitherapy, J. Comput. Appl. Math. 263 (2014), 326–337.

[26] C. Ding, N. Tao, Y. Zhu, A mathematical model of Zika virus and its optimal control, in: 2016 35th Chinese Control Conference (CCC), IEEE, Chengdu, China, 2016: pp. 2642–2645.

[27] B.N. Kim, K. Nah, C. Chu, S.U. Ryu, Y.H. Kang, Y. Kim, Optimal Control Strategy of Plasmodium vivax Malaria Transmission in Korea, Osong Public Health Res. Perspect. 3 (2012), 128–136.

[28] O. Prosper, N. Ruktanonchai, M. Martcheva, Optimal vaccination and bednet maintenance for the control of malaria in a region with naturally acquired immunity, J. Theor. Biol. 353 (2014), 142–156.

[29] I. Elmouki, S. Saadi, Quadratic and linear controls developing an optimal treatment for the use of bcg immunotherapy in superficial bladder cancer, Opt. Control Appl. Meth. 37 (1) (2016), 176–189.

[30] U. Ledzewicz, H. Schättler, Antiangiogenic therapy in cancer treatment as an optimal control problem, SIAM J. Control Optim. 46 (3) (2007), 1052–1079.

[31] E. Jung, S. Lenhart, Z. Feng, Optimal control of treatments in a two-strain tuberculosis model, Discrete Contin. Dyn. Syst. B. 2 (4) (2002), 473.

[32] D. P. Moualeu, M. Weiser, R. Ehrig, P. Deuflhard, Optimal control for a tuberculosis model with undetected cases in cameroon, Commun. Nonlinear Sci. Numer. Simul. 20 (3) (2015), 986–1003.

[33] Y. Su, D. Sun, Optimal control of anti-hbv treatment based on combination of traditional chinese medicine and western medicine, Biomed. Signal Process. Control. 15 (2015), 41–48.

[34] J. Lowden, R. M. Neilan, M. Yahdi, Optimal control of vancomycin-resistant enterococci using preventive care and treatment of infections, Math. Biosci. 249 (2014), 8–17.

[35] I. Abouelkheir, M. Rachik, O. Zakary, I. Elmouk, A multi-regions sis discrete influenza pandemic model with a travel-blocking vicinity optimal control approach on cells, Amer. J. Comput. Appl. Math 7 (2) (2017), 37–45.

[36] L. Abu-Raddad, F. A. Akala, I. Semini, G. Riedner, D. Wilson, O. Tawil, Characterizing the HIV/AIDS epidemic in the Middle East and North Africa: time for strategic action, The World Bank, 2010.

[37] D. Bundy, A. Patrikios, C. Mannathoko, A. Tembon, S. Manda, B. Sarr, L. Drake, Accelerating the education sector response to HIV: Five years of experience from Sub-Saharan Africa, The World Bank, Washington, 2010.

[38] L. S. Pontryagin, Mathematical theory of optimal processes, Routledge, 2018.

[39] Nouveau découpage territorial du royaume?, http://www.pncl.gov.ma/fr/News/Alaune/Pages/Nouveau-d%C3%A9coupage-r%C3%A9gional-du-Royaume-.aspx (2015).

[40] Recensement general de la population et de l'habitat 2014, https://www.hcp.ma/reg-casablanca/attachment/673830/ (2015).

[41] La région de rabat-salé-kénitra, http://www.pncl.gov.ma/fr/LesCollectivit%C3%A9sterritoriales/Documents/MONOGRAPHIE%20DE%20LA%20REGION%20DE%20RABAT%20SALE%20%20KENITRA%20FR.pdf (2015).

[42] What is a shapefile? https://desktop.arcgis.com/en/arcmap/latest/manage-data/shapefiles/what-is-a-shapefile.htm (2020).

[43] What is arcmap? https://desktop.arcgis.com/fr/arcmap/10.3/main/map/what-is-arcmap-.htm (2020).

[44] An overview of the neighborhood tools, https://desktop.arcgis.com/en/arcmap/10.3/tools/spatial-analyst-toolbox/an-overview-of-the-neighborhood-tools.htm (2020).